
Article:
Pessu, F orcid.org/0000-0003-3587-4309, Barker, R orcid.org/0000-0002-5106-6929 and Neville, A orcid.org/0000-0002-6479-1871 (2017) Pitting and uniform corrosion of X65 carbon steel in sour corrosion environments: The influence of CO2, H2S and temperature. CORROSION, 73 (9). pp. 1168-1183. ISSN 0010-9312

https://doi.org/10.5006/2454

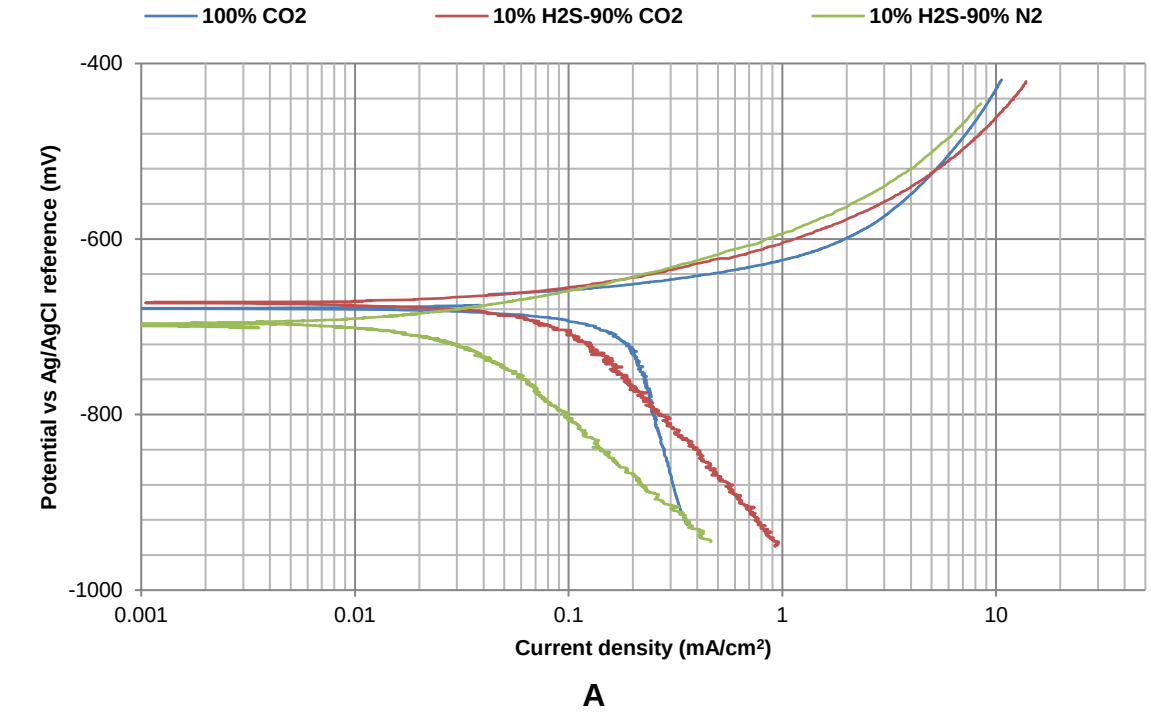

A

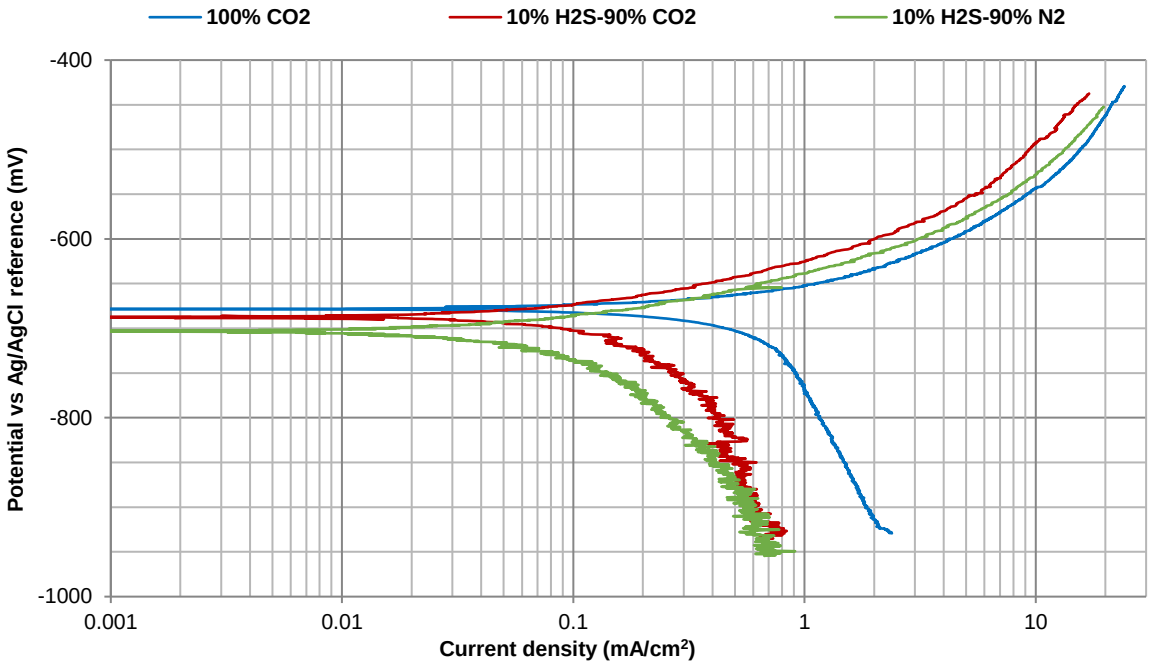

B

FIGURE 1: Tafel polarization plots for X65 carbon steel in 3.5 wt.% NaCl solution saturated with 100 mol.% CO_2, 10 mol.% H_2S-90 mol.% CO_2 and 10 mol.% H_2S-90 mol.% N_2 at (a) 30℃ and (b) 80℃ after 7 h exposure.

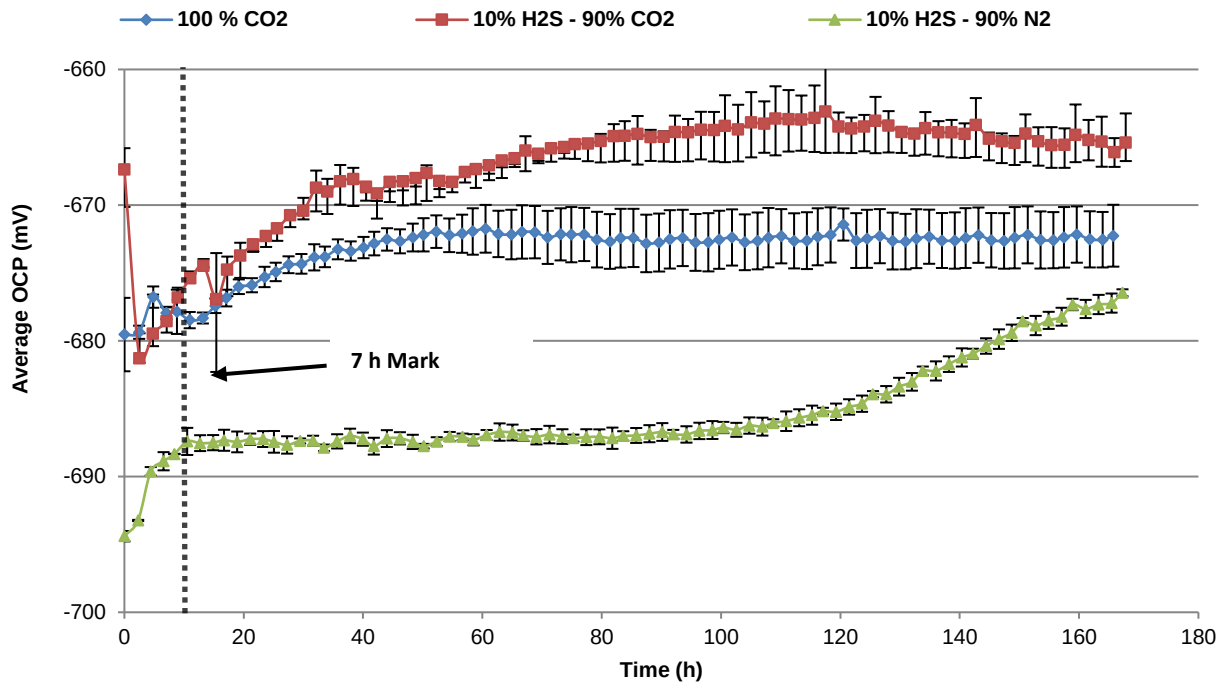

A

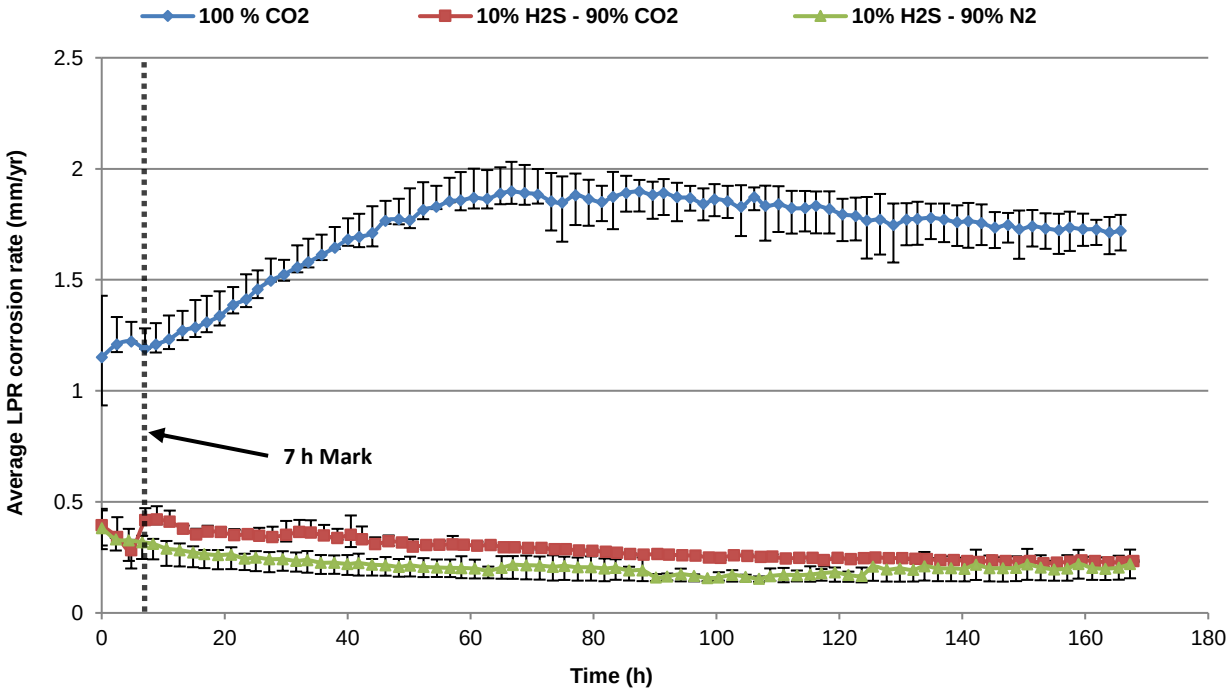

B

Figure 2: Graphs of (a) corrosion potential and (b) corrosion rate of X65 carbon steel in 3.5 wt. % NaCl solution under three different gas atmospheres at 30℃, ove r 168 h.

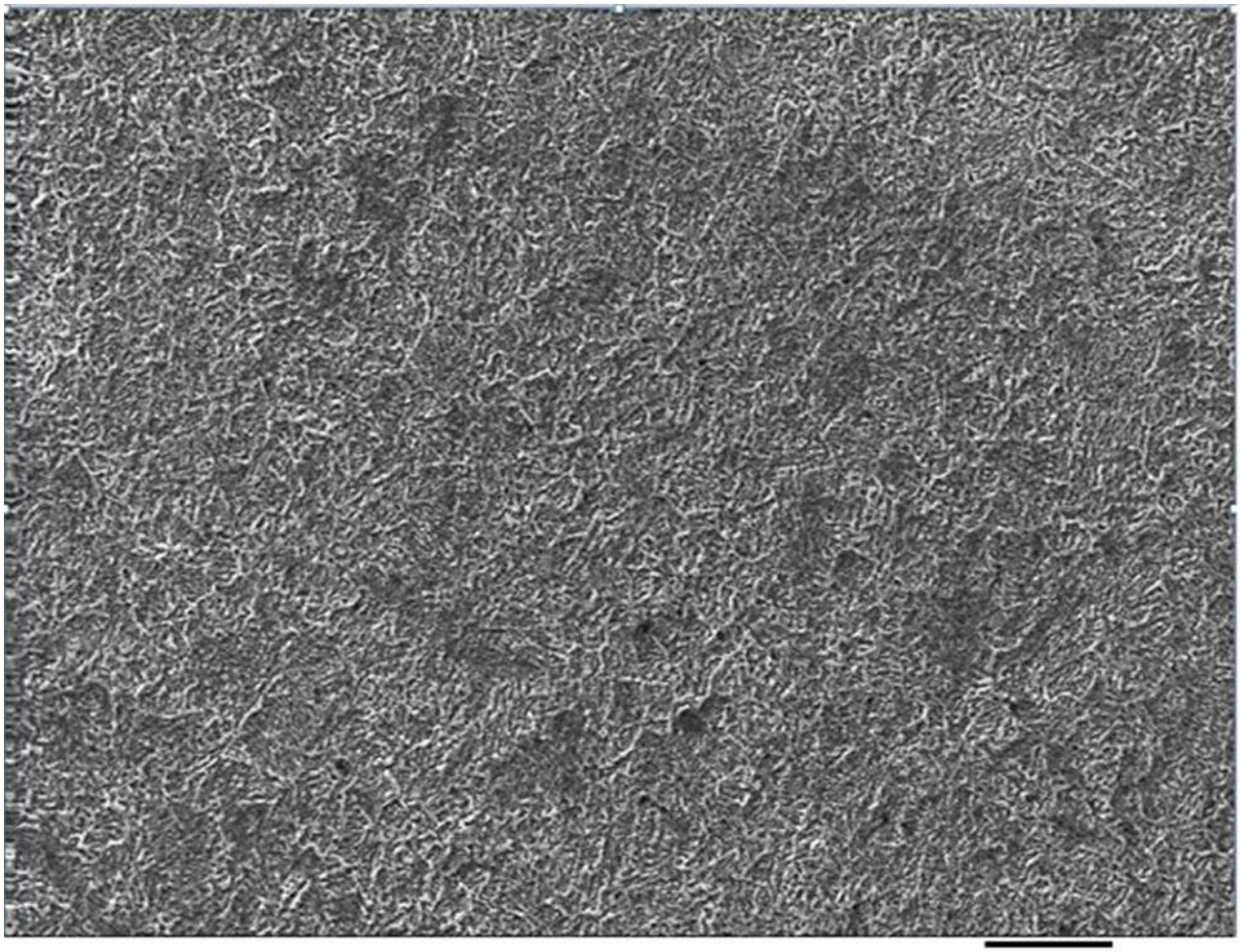

A

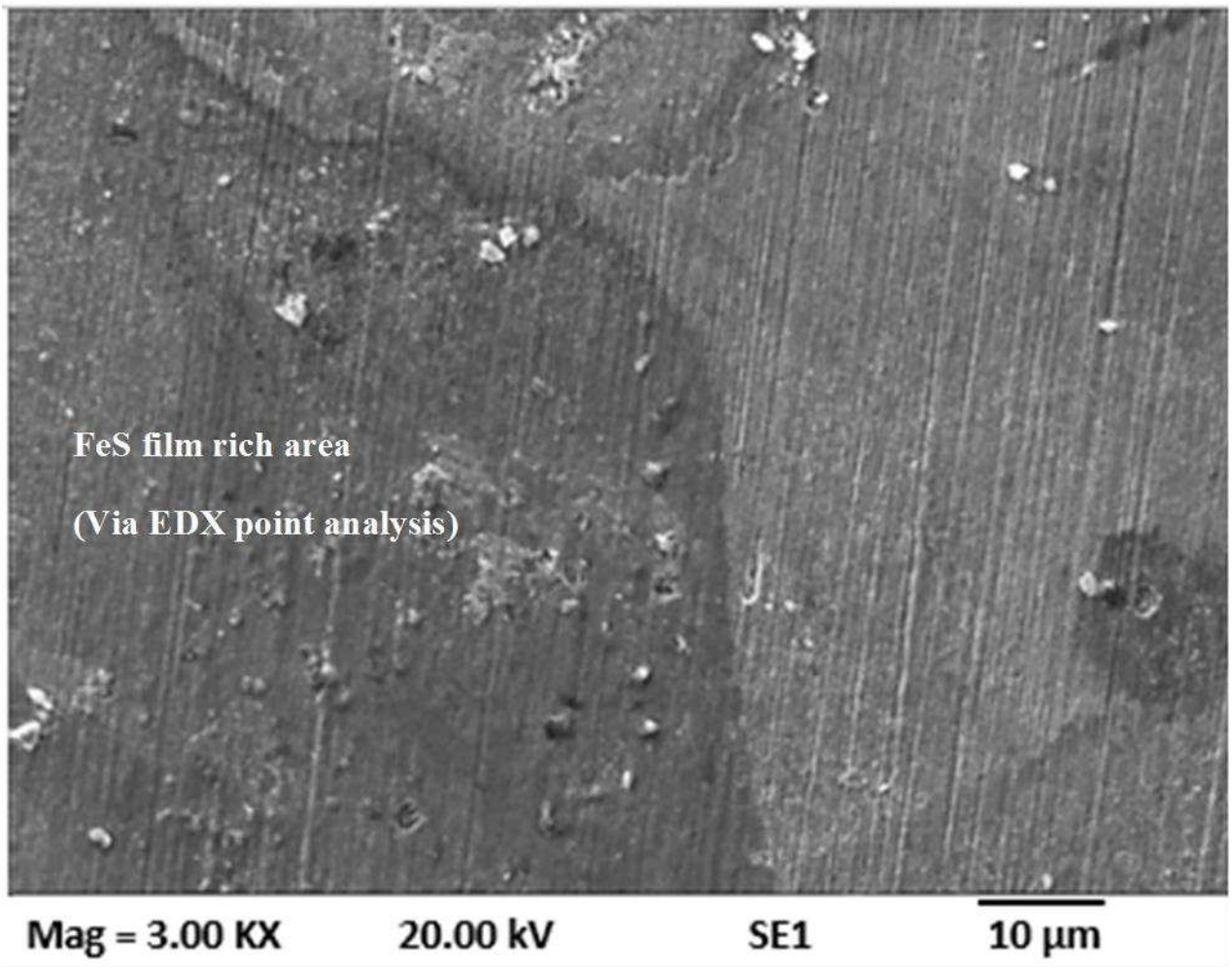
FeS film rich area
(Via EDX point analysis)
Mag = 3.00 KX
20.00 kV
SE1
10 µm

B

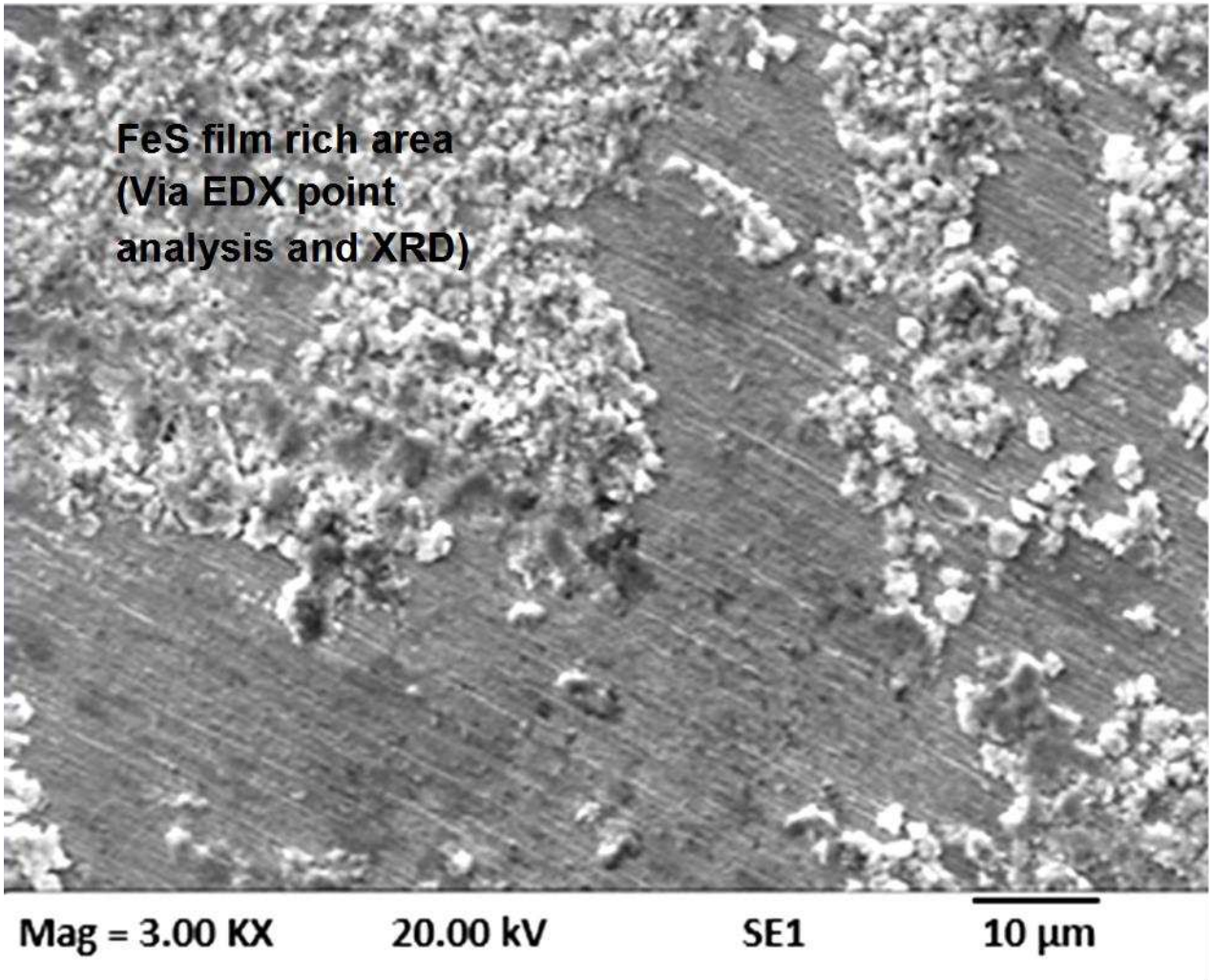
FeS film rich area
(Via EDX point
analysis and XRD)
Mag = 3.00 KX
20.00 kV
SE1
10 µm

C

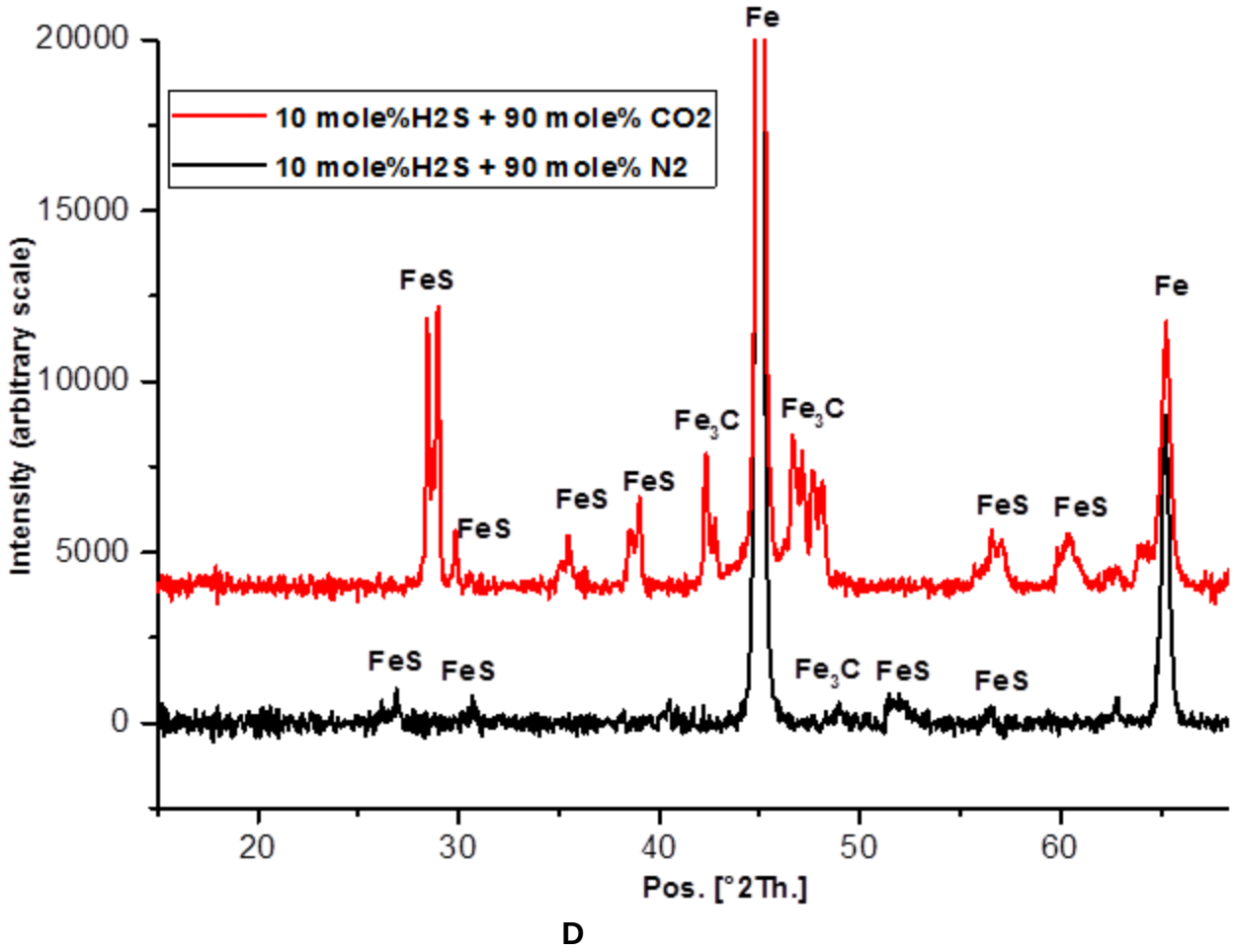

Figure 3: SEM images of corrosion product layer on X65 carbon steel in 3.5 wt.% NaCl solution saturated with (a) 100 mol.% CO_2, (b) 10 mol.% H_2S- 90 mol.% CO_2 and (c) 10 mol.% H_2S-90 mol.% N_2 at 30℃. (d) XRD pattern for corrosion product layer on X65 carbon steel in 3.5 wt.% NaCl solution saturated 10 mol.% H_2S- 90 mol.% CO_2 and 10 mol.% H_2S-90 mol.% N_2 at 30℃. Images are for test duration of 7 h. (Note that the intensity scale is arbitrary).

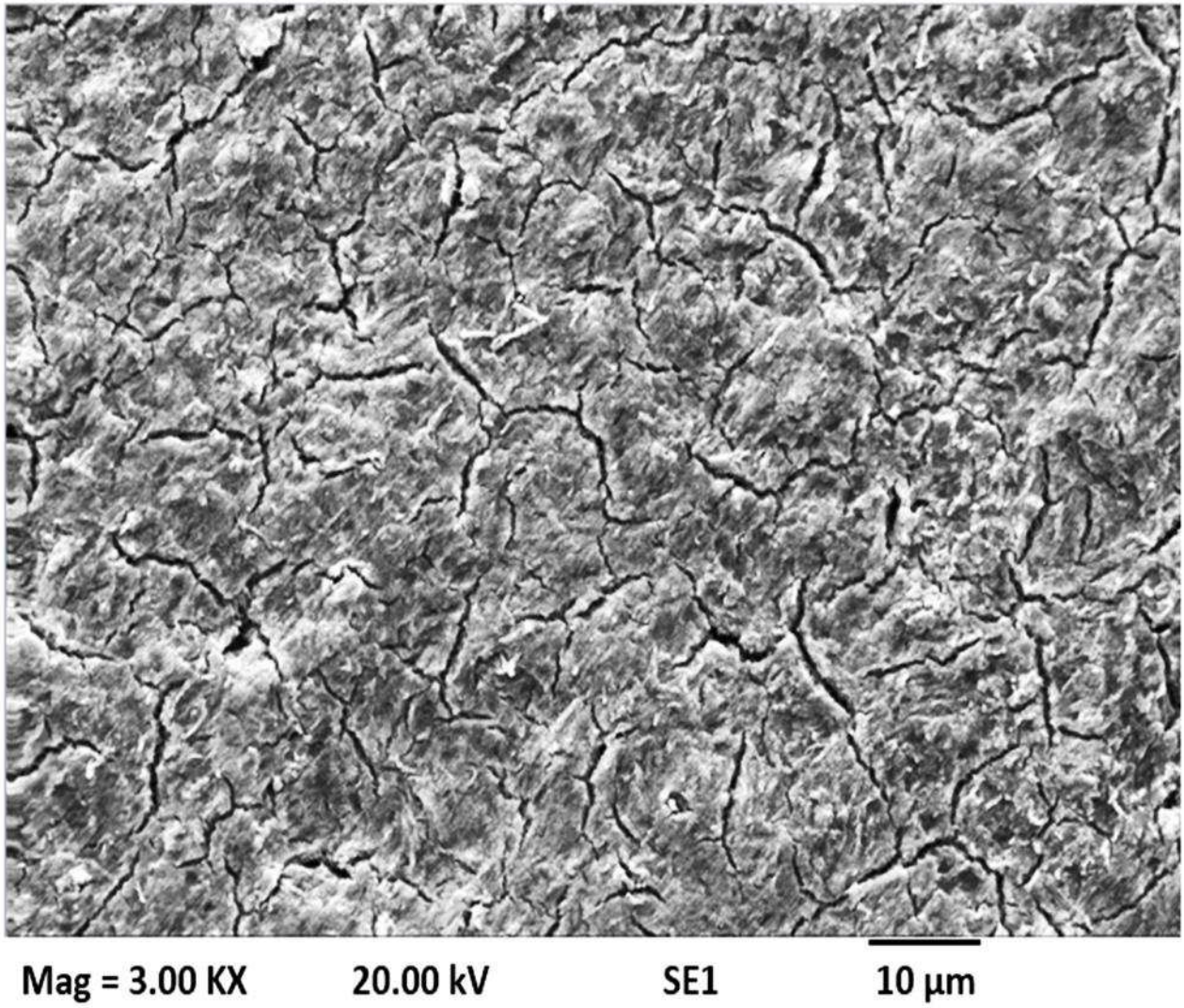

A

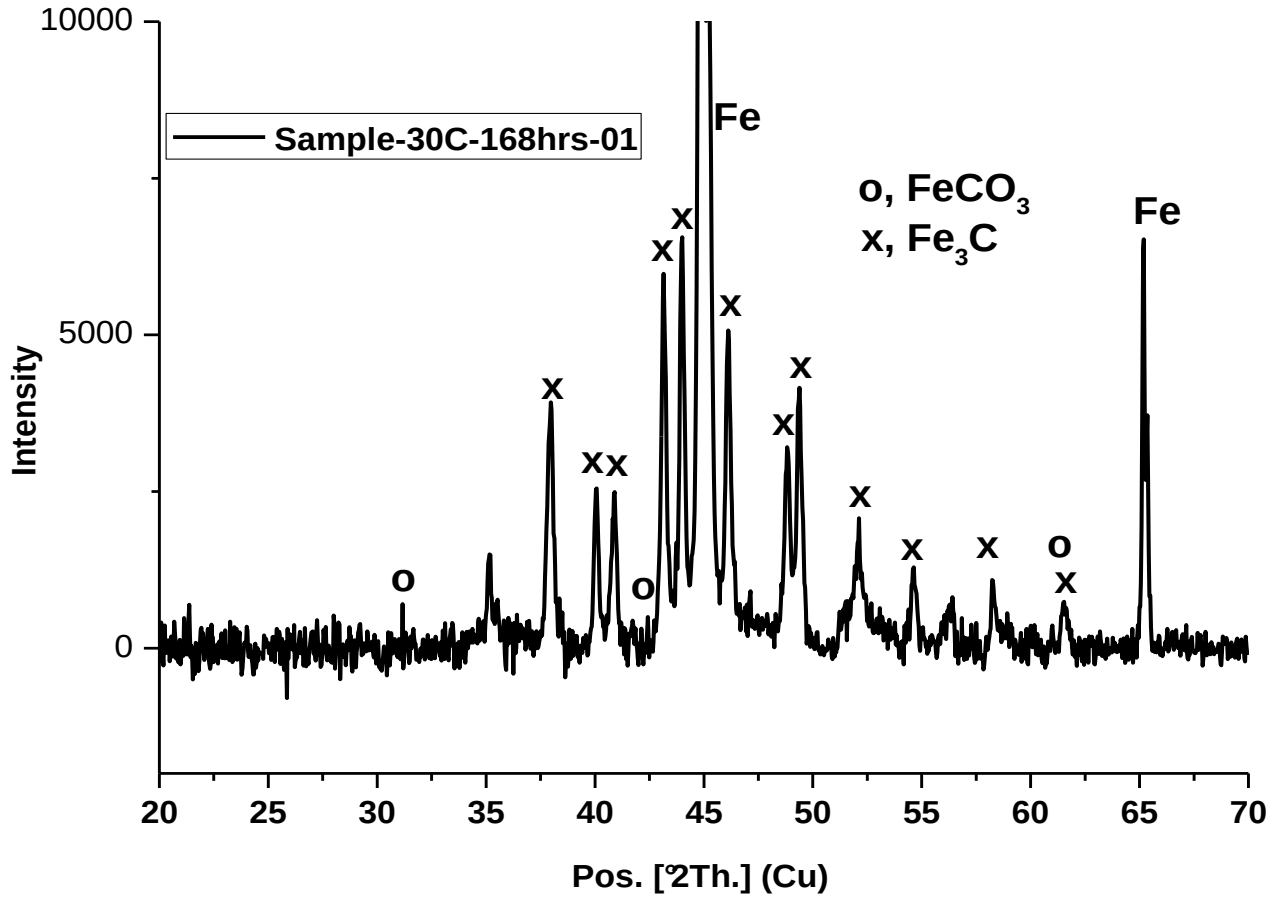
10000
5000
0
Intensity
Sample-30C-168hrs-01
Fe
o, FeCO3
x, Fe3C
Fe
20
25
30
35
40
45
50
55
60
65
70
Pos. [°2Th.] (Cu)

B

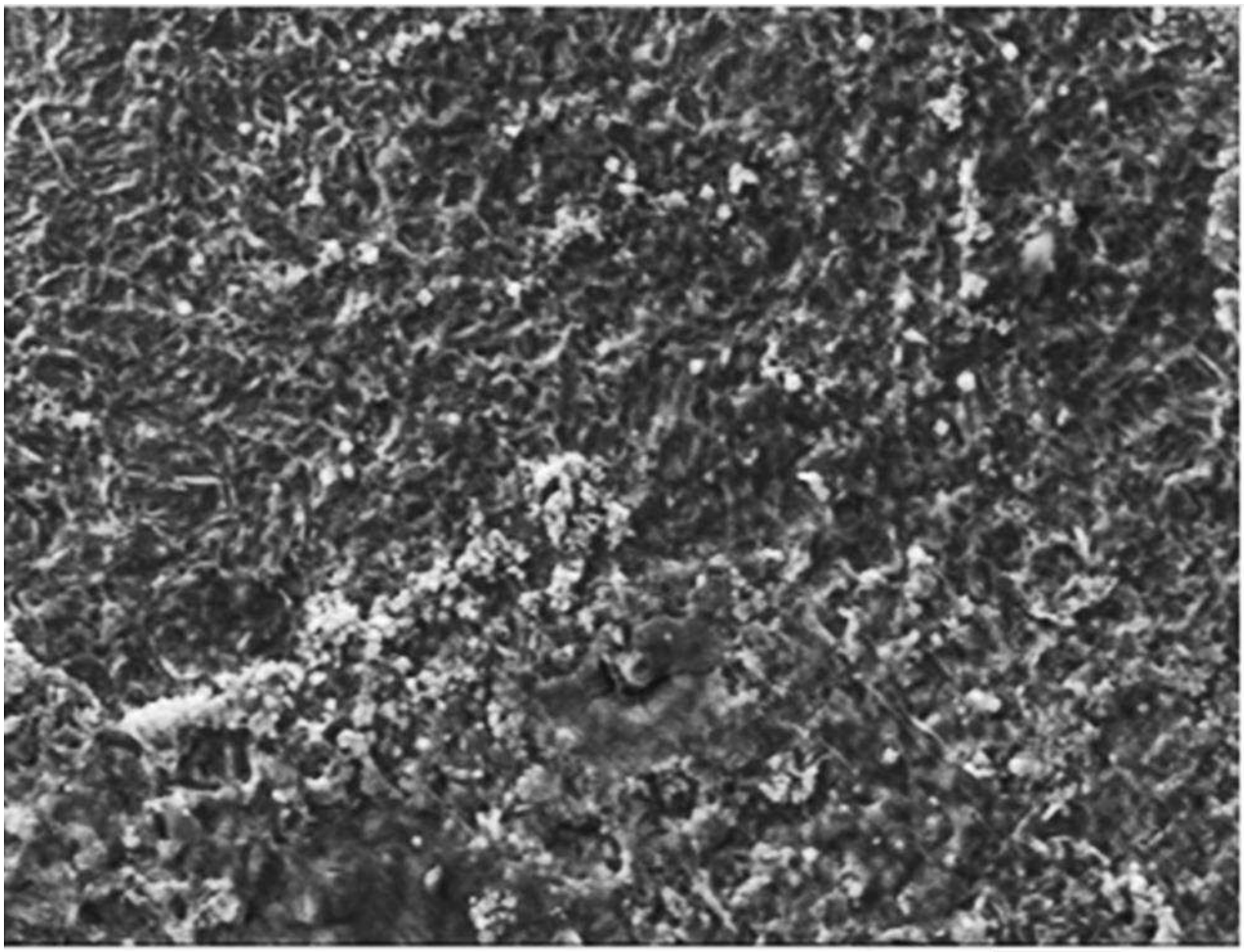

C

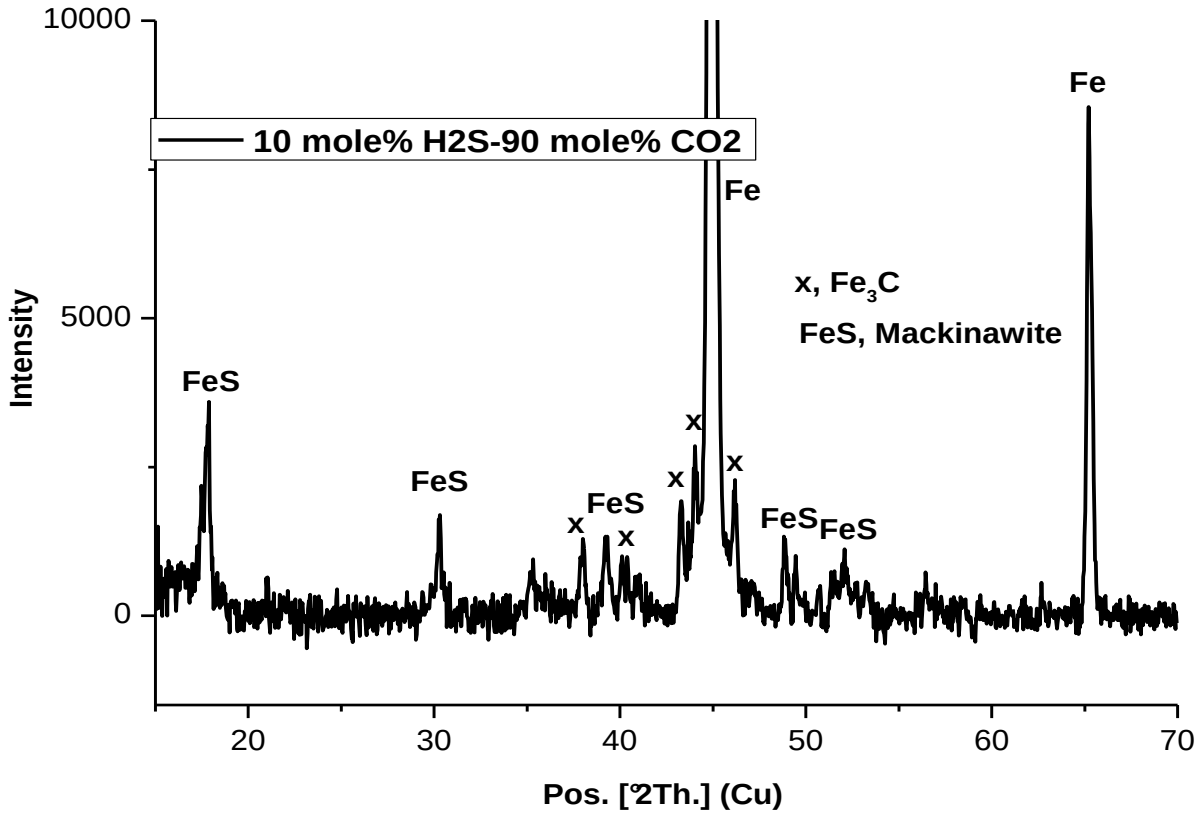
10000
5000
0
Intensity
10 mole% H2S-90 mole% CO2
Fe
x, Fe3C
FeS, Mackinawite
FeS
FeS
FeS
FeS
FeS
Fe
x
x
x
x
20
30
40
50
60
70
Pos. [°2Th.] (Cu)

D

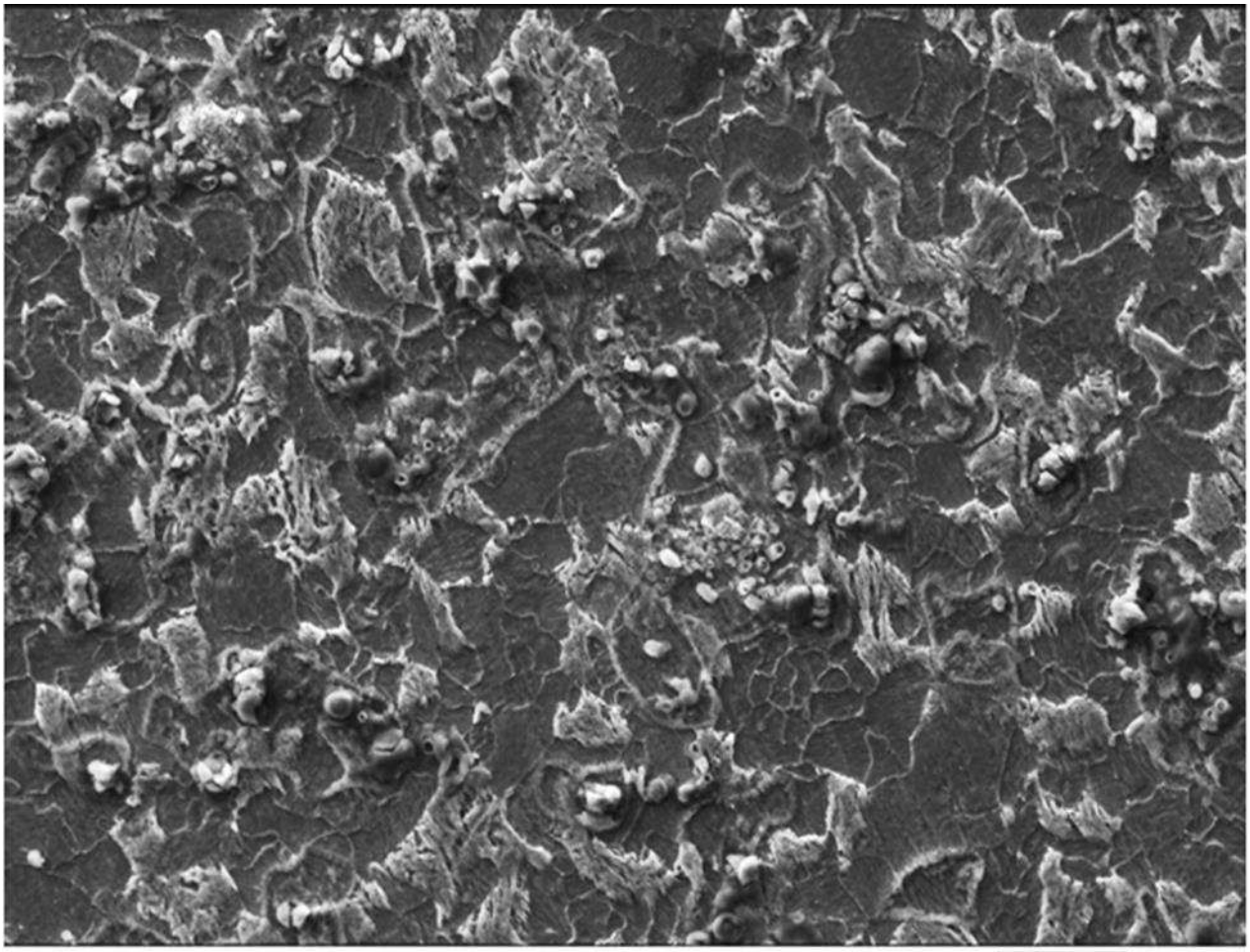

E

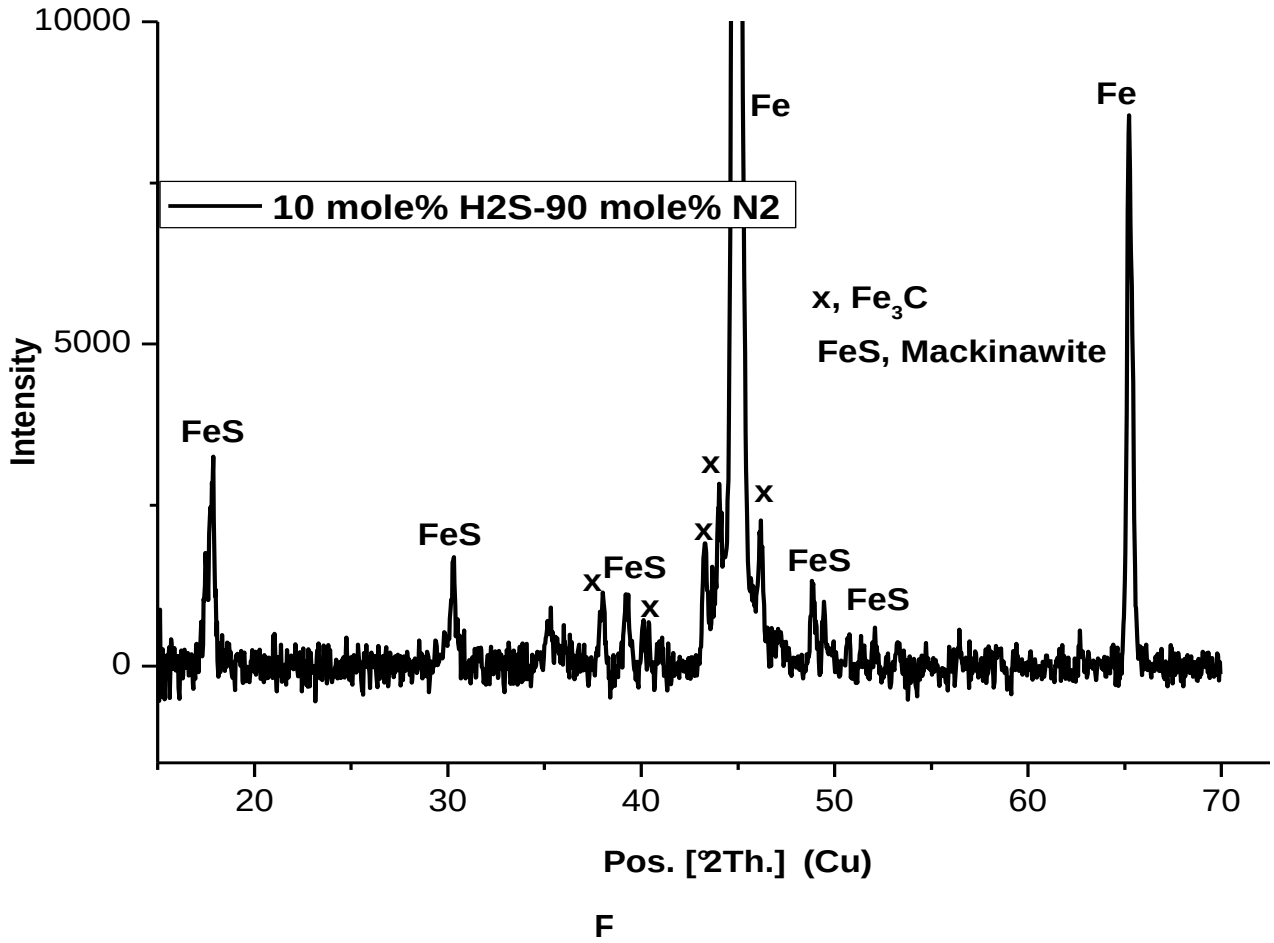

F

Figure 4: SEM images and XRD patterns of corrosion product layer on X65 carbon steel in 3.5 wt.% NaCl solution under gas atmospheres composed of (a) 100 mol.% CO_2, (b) XRD pattern for 100 mol.% CO_2 (c) 10 mol.% H_2S- 90 mol.%CO_2 (d) XRD pattern for 10 mol.% H_2S- 90 mol.%CO_2 (e) 10 mol.% H_2S-90 mol.% N_2 and (f) 10 mol.% H_2S-90 mol.% N_2 at 30℃ and after 168 h.

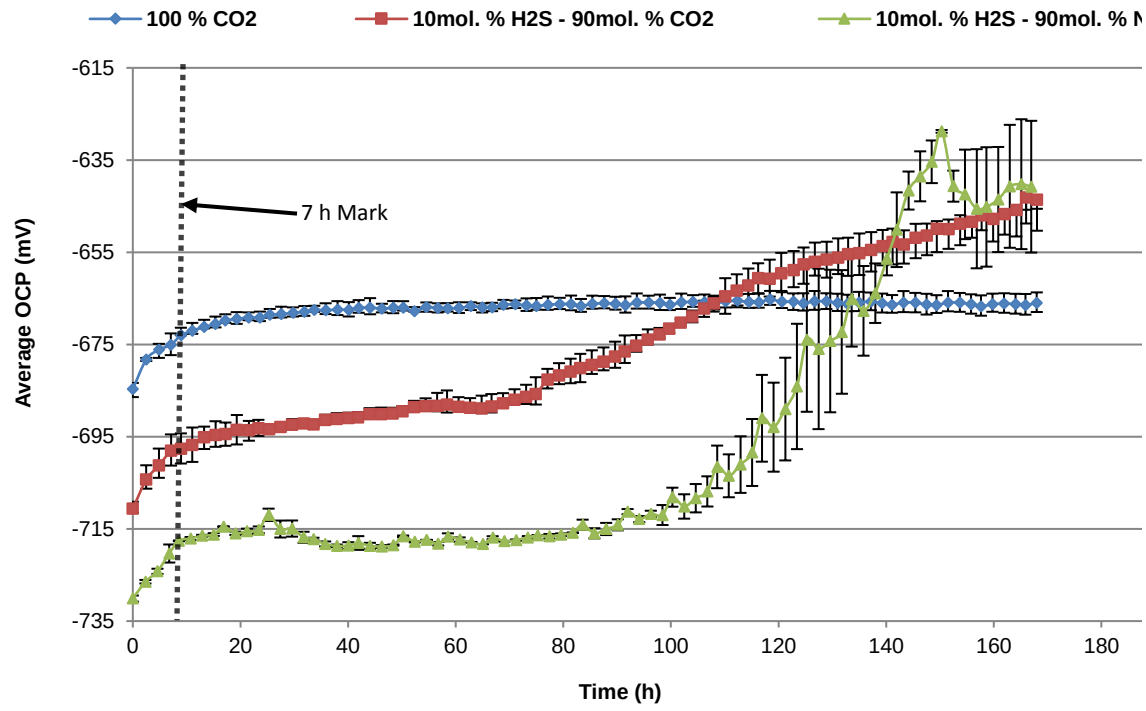

A

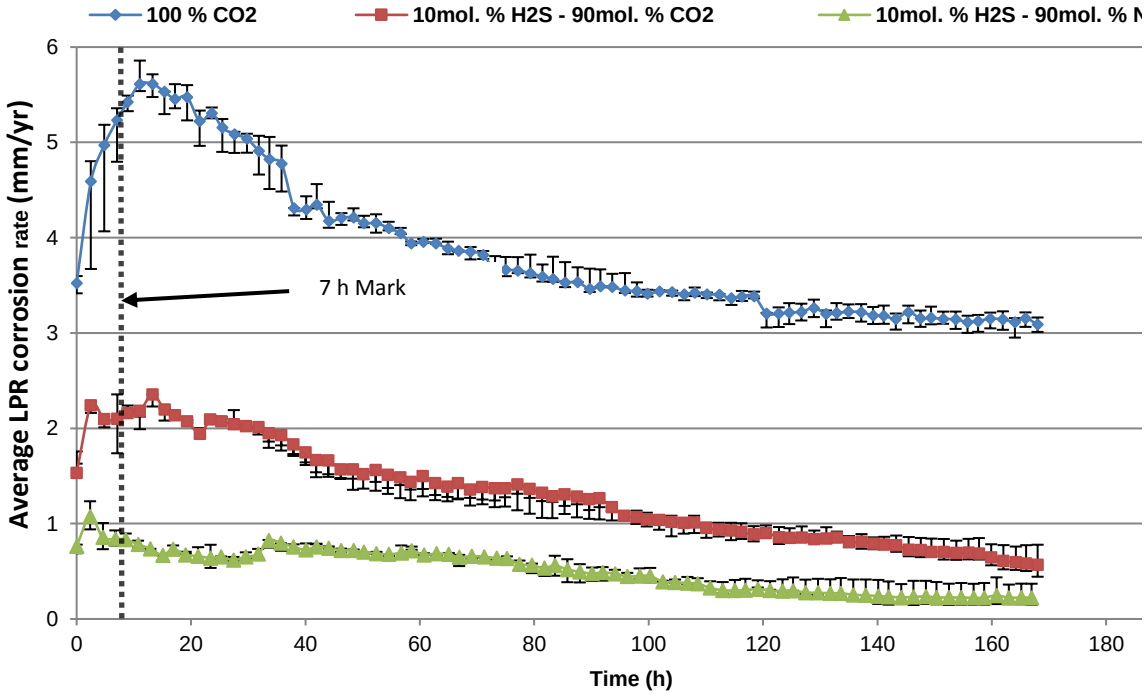

B

Figure 5: Graphs of (a) corrosion potential and (b) corrosion rate of X65 carbon steel in 3.5 wt. % NaCl solution under three different gas atmospheres at 80˚C, over 168 h.

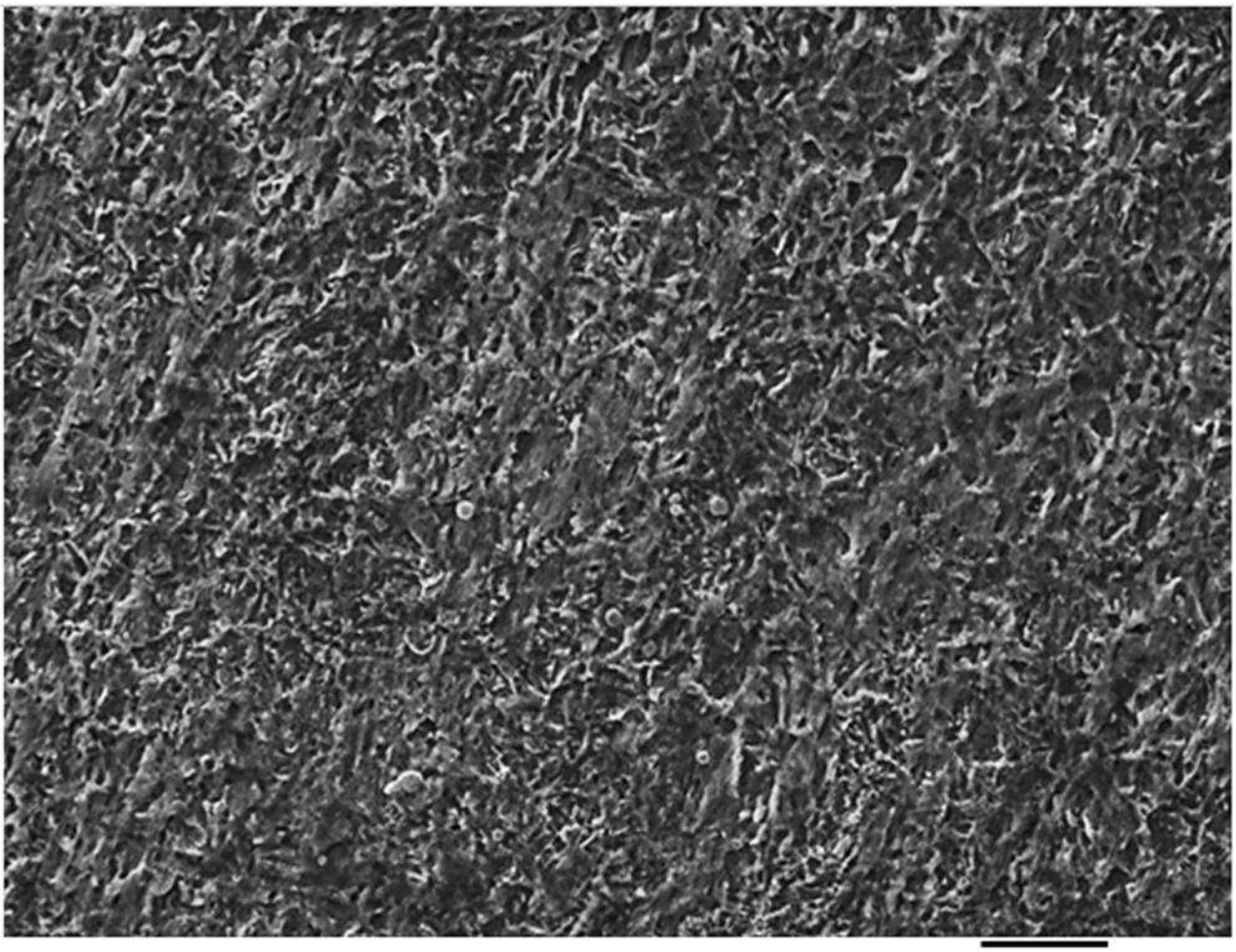

A

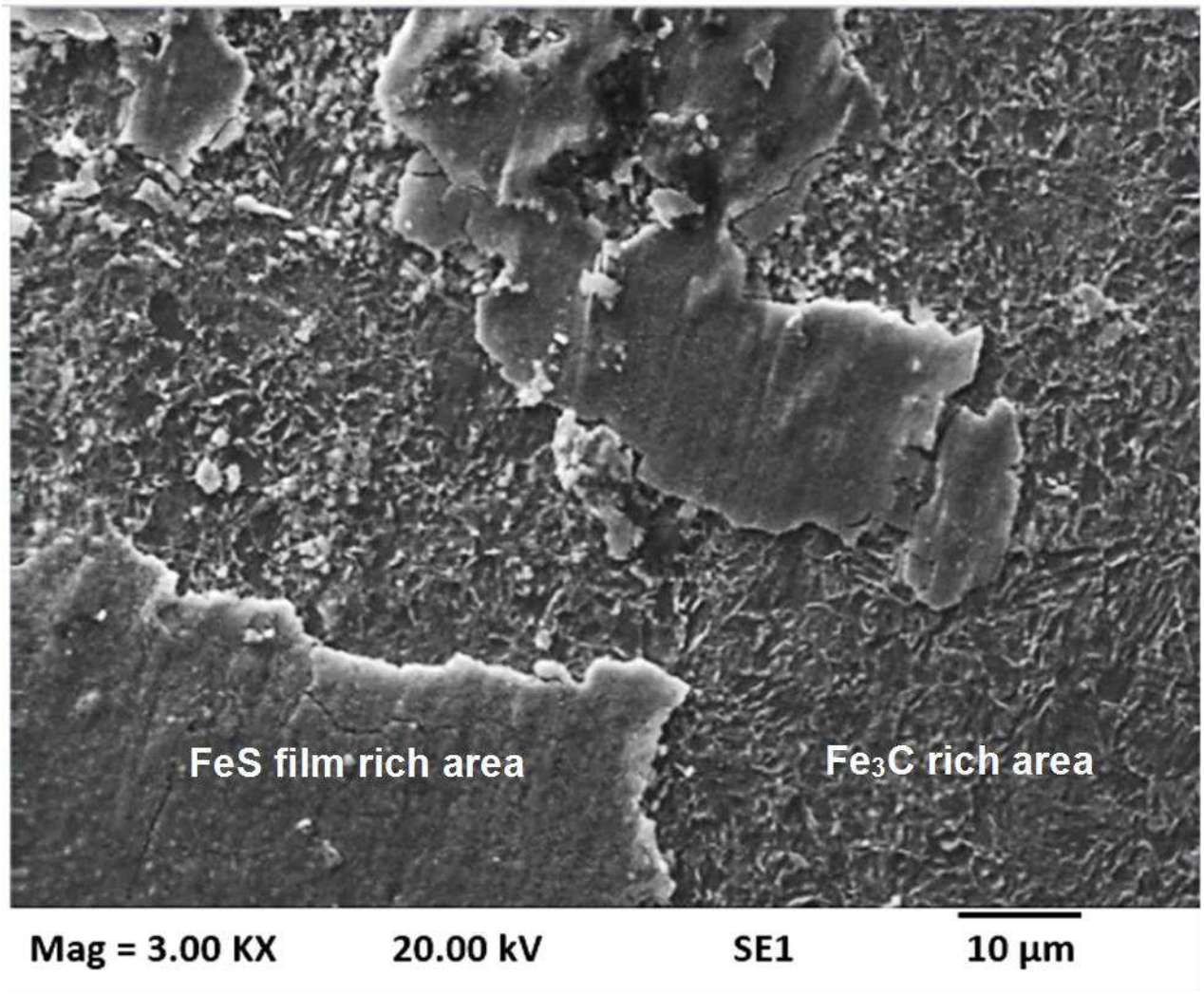

6B

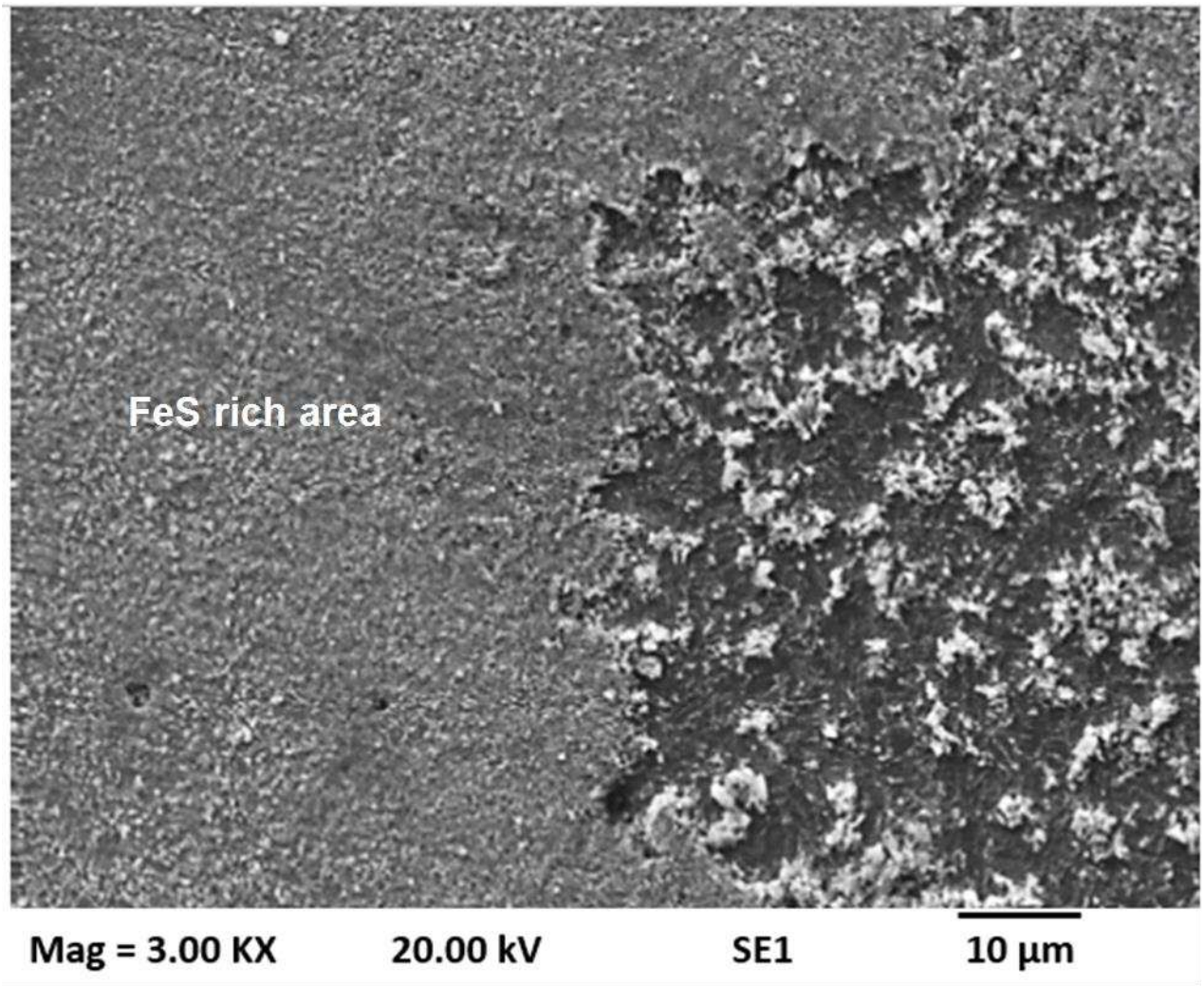

C

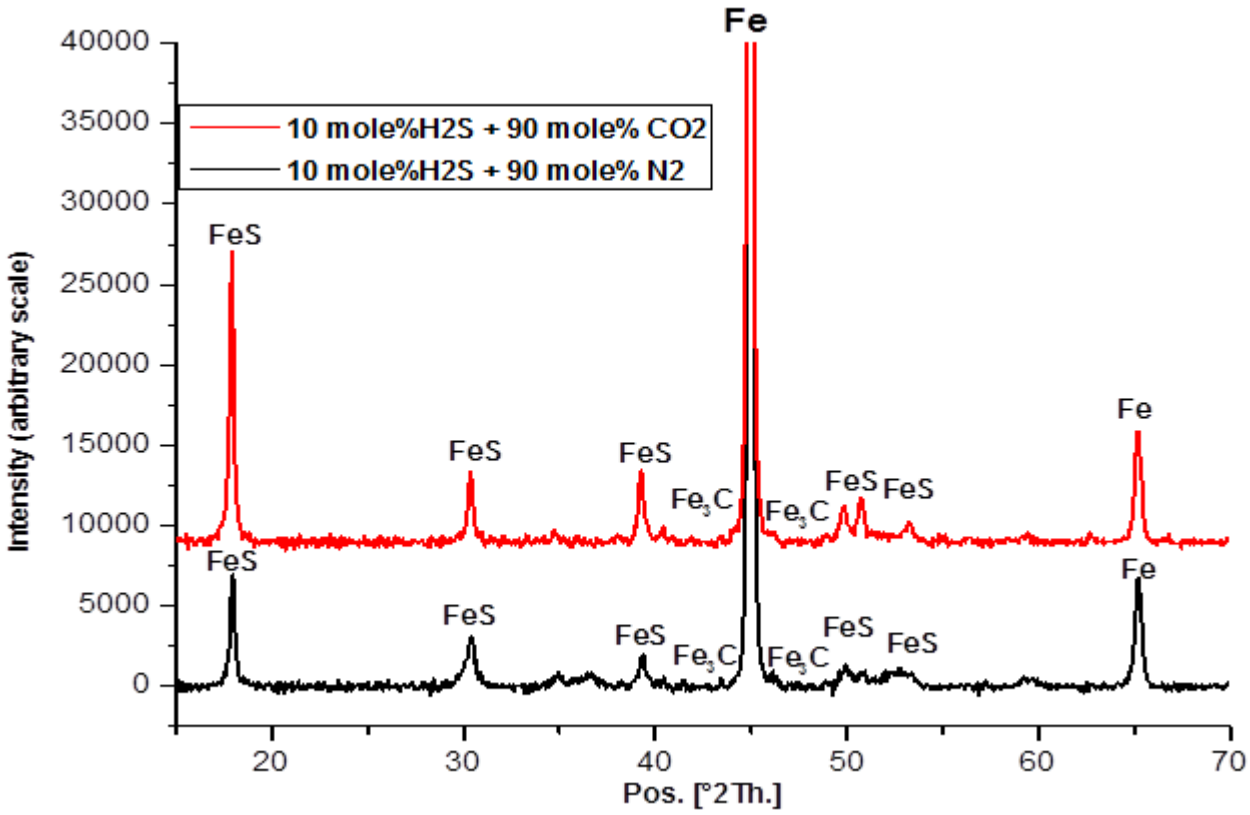

D

Figure 6: SEM images of corrosion product layer on X65 carbon steel in 3.5 wt.% NaCl solution saturated with (a) 100 mol.% CO_2, (b) 10 mol.% H_2S- 90 mol.% CO_2 and (c) 10 mol.% H_2S-90 mol.% N_2 at 80℃. (d) XRD pattern for corrosion product layer on X65 carbon steel in 3.5 wt.% NaCl solution saturated 10 mol.% H_2S- 90 mol.% CO_2 and 10 mol.% H_2S-90 mol.% N_2 at 80℃ for test after 7 h. (The intensity scale is arbitrary).

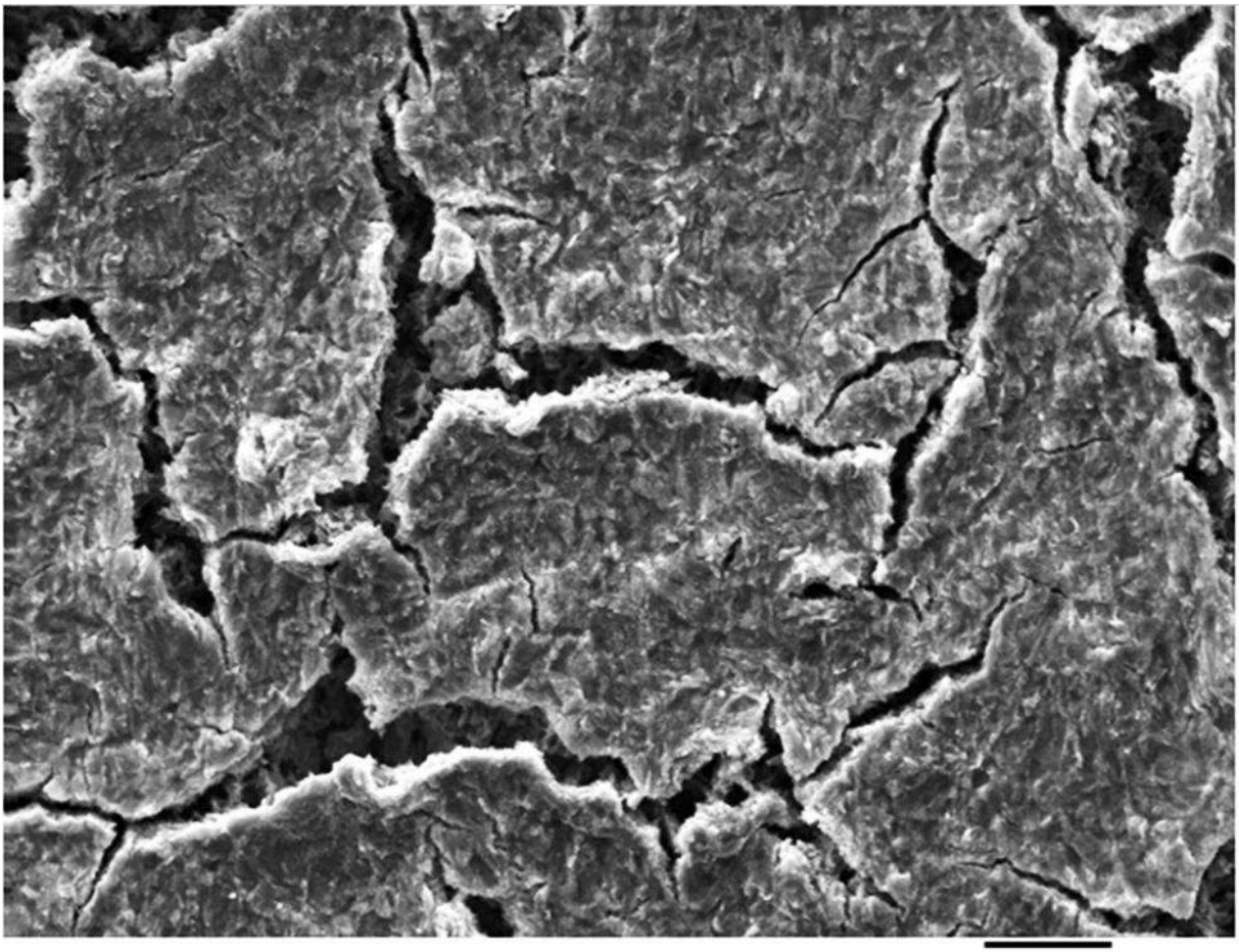

A

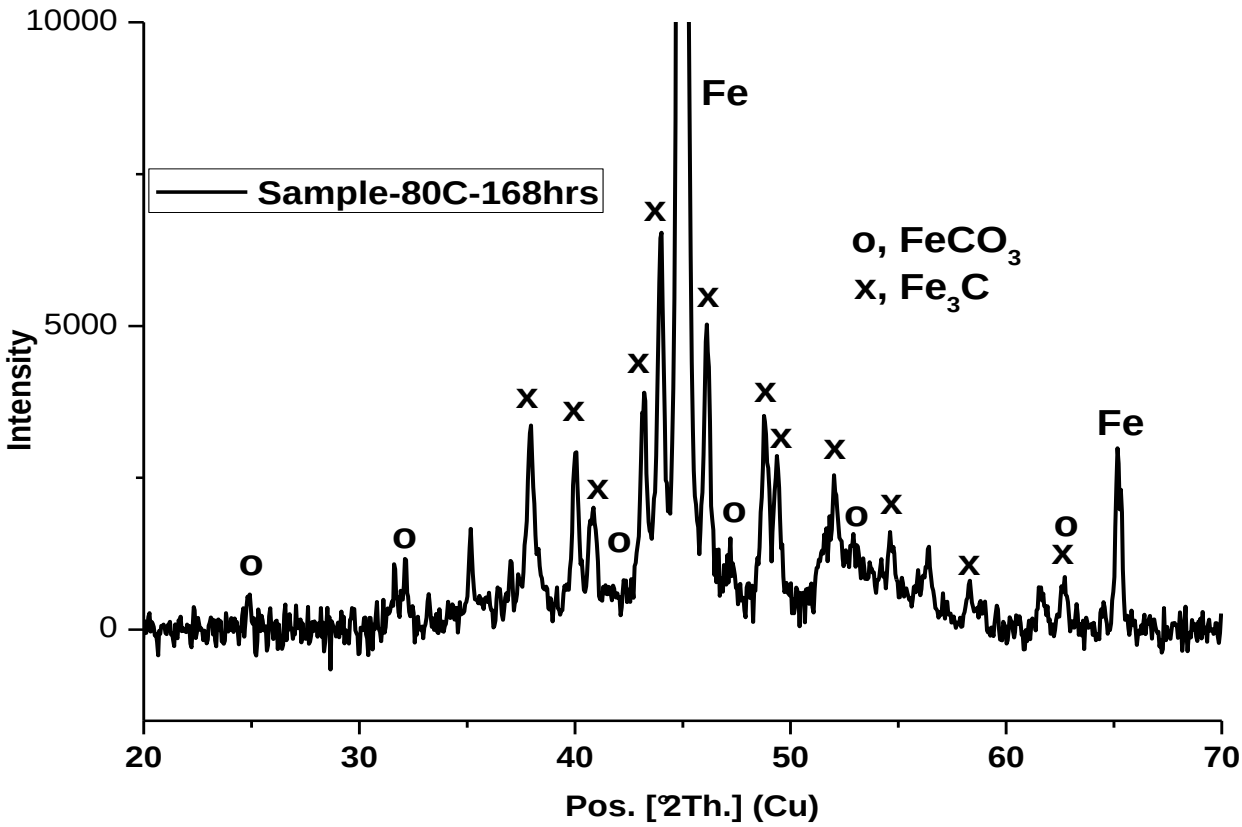
10000
5000
0
Intensity
Sample-80C-168hrs
o, FeCO3
x, Fe3C
Fe
Fe
20
30
40
50
60
70
Pos. [°2Th.] (Cu)

B

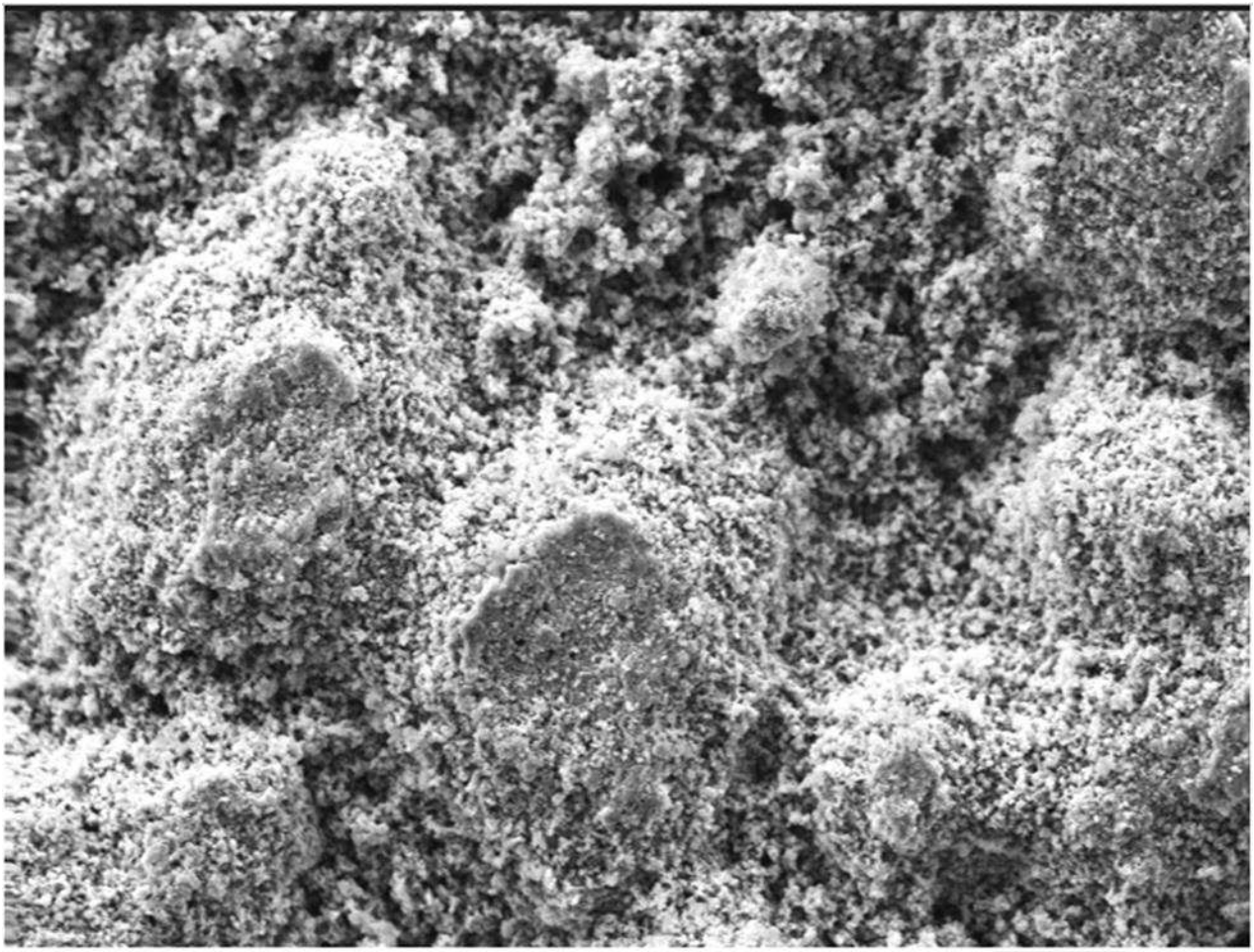

C

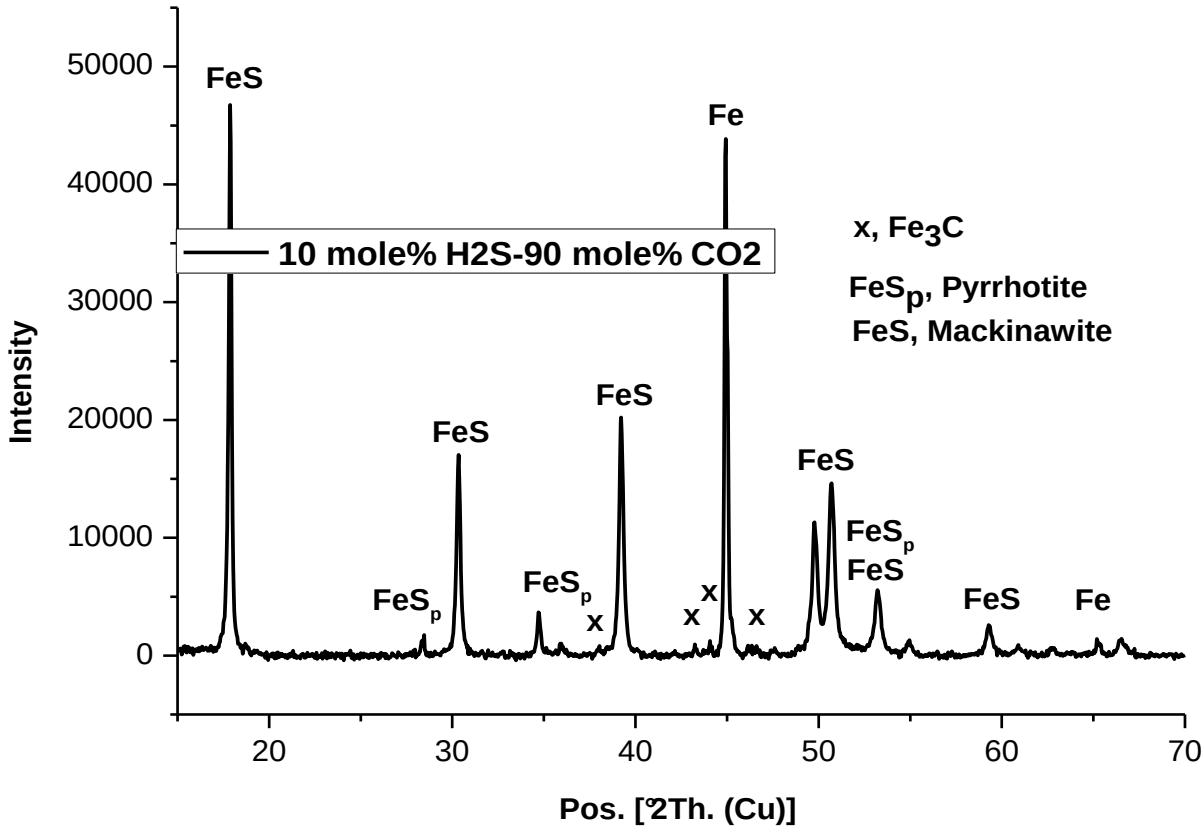
50000
40000
30000
20000
10000
0
Intensity
10 mole% H2S-90 mole% CO2
x, Fe3C
FeSp, Pyrrhotite
FeS, Mackinawite
FeS
Fe
FeSp
x
20
30
40
50
60
70
Pos. [°2Th. (Cu)]

D

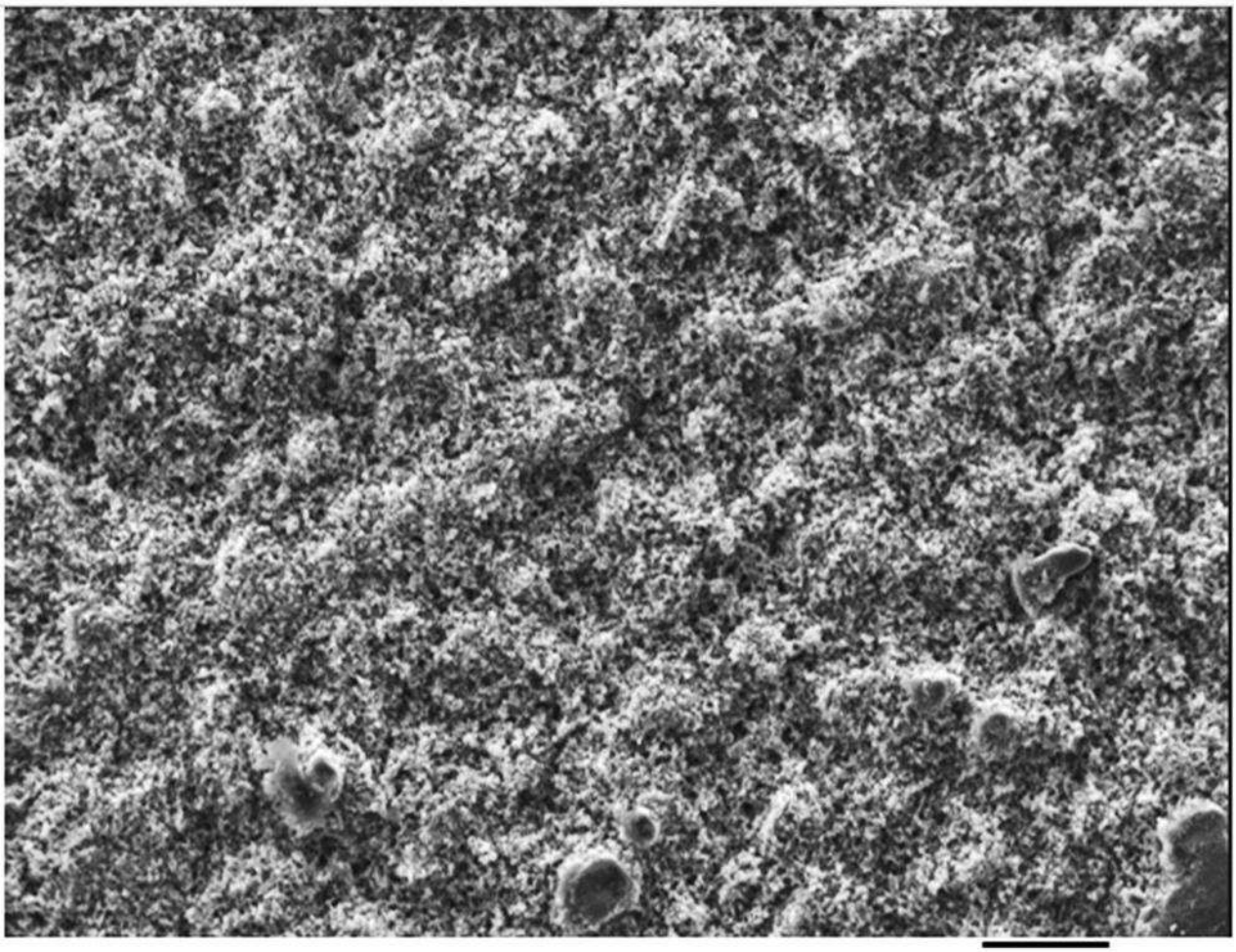

E

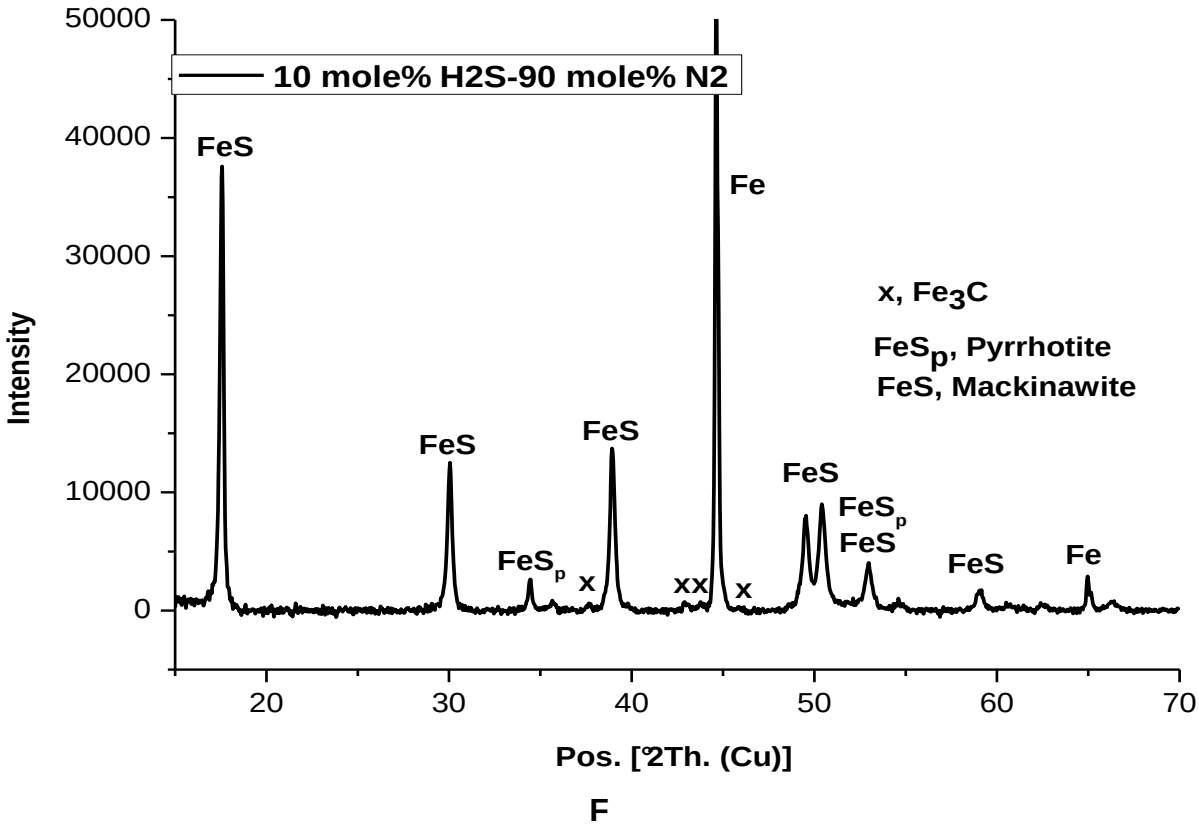

F

Figure 7: SEM images and XRD patterns of corrosion product layer on X65 carbon steel in 3.5 wt.% NaCl solution under gas atmospheres composed of (a) 100 mol.% CO_2, (b) XRD pattern for 100 mol.% CO_2 (c) 10 mol.% H_2S- 90 mol.%CO_2 (d) XRD pattern for 10 mol.% H_2S- 90 mol.% CO_2 (e) 10 mol.% H_2S-90 mol.% N_2 and (f) 10 mol.% H_2S-90 mol.% N_2 at 80℃ and after 168 h.

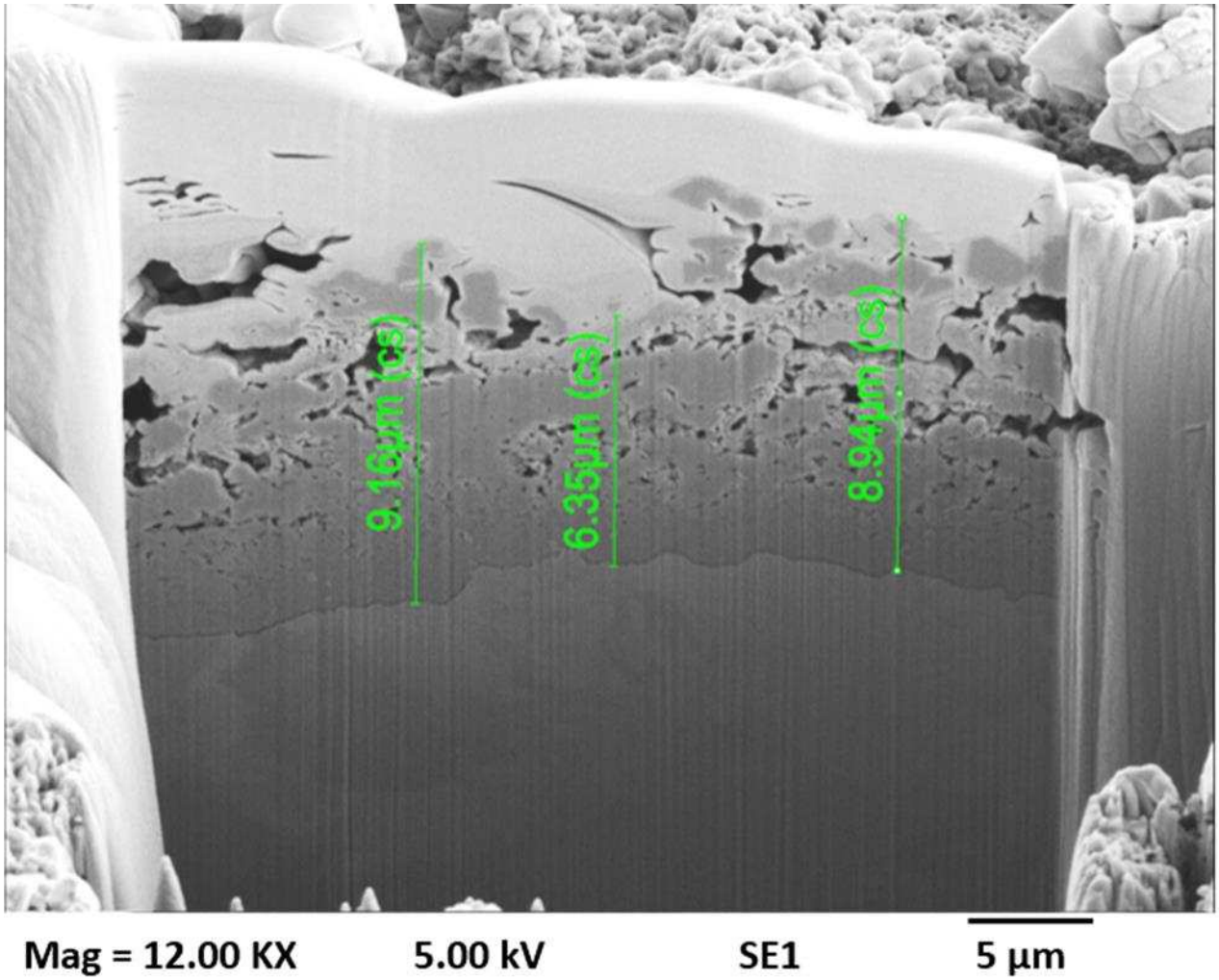

A

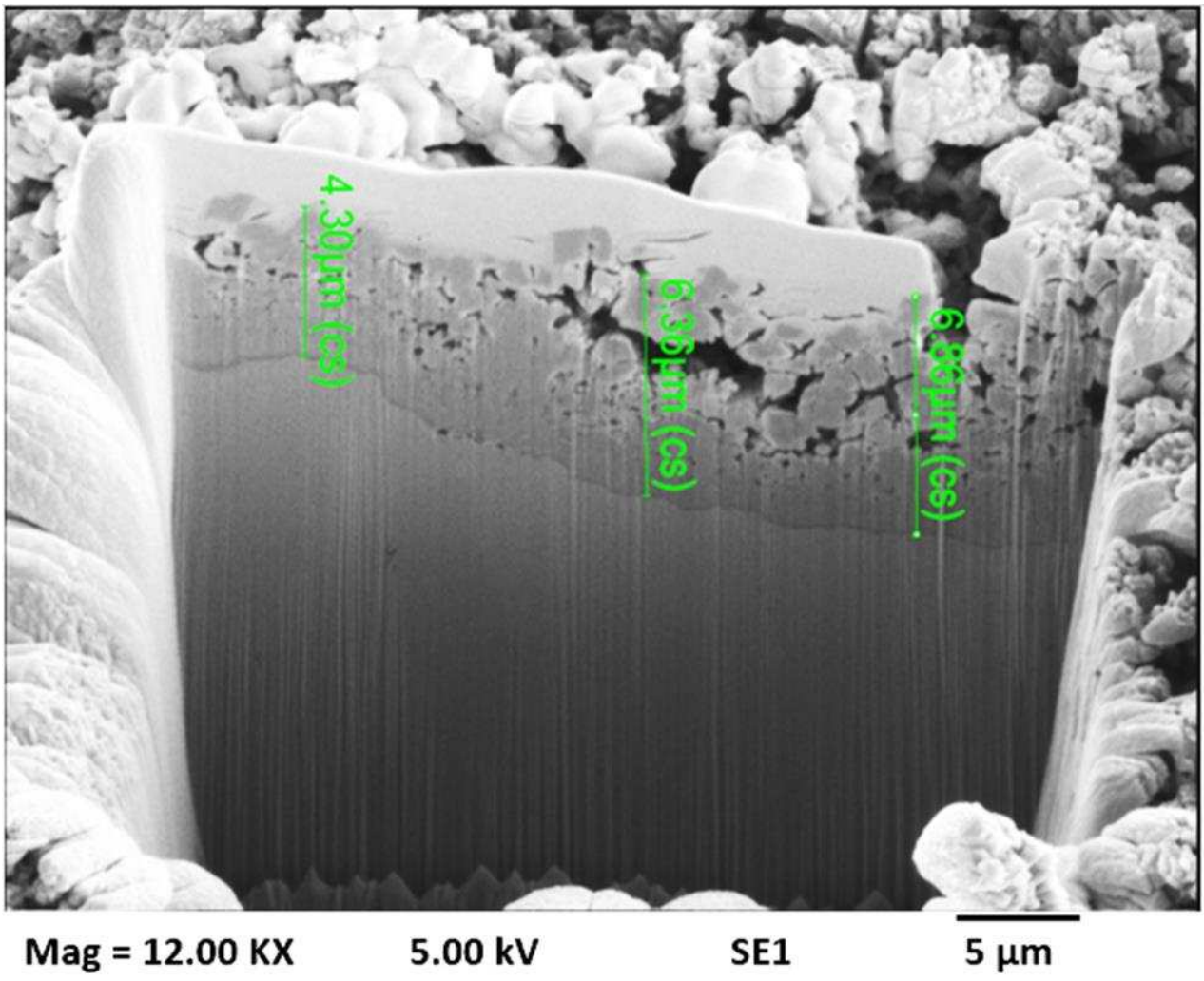

B

Figure 8: Cross-sectional view after micro-machining using the FIB for (a) SEM image shown in Figure 13(c) for 10 mol.% H_2S- 90 mol.% CO_2 and (b) SEM image shown in Figure 13(e) for 10 mol.% H_2S- 90 mol.% N_2 at 80℃

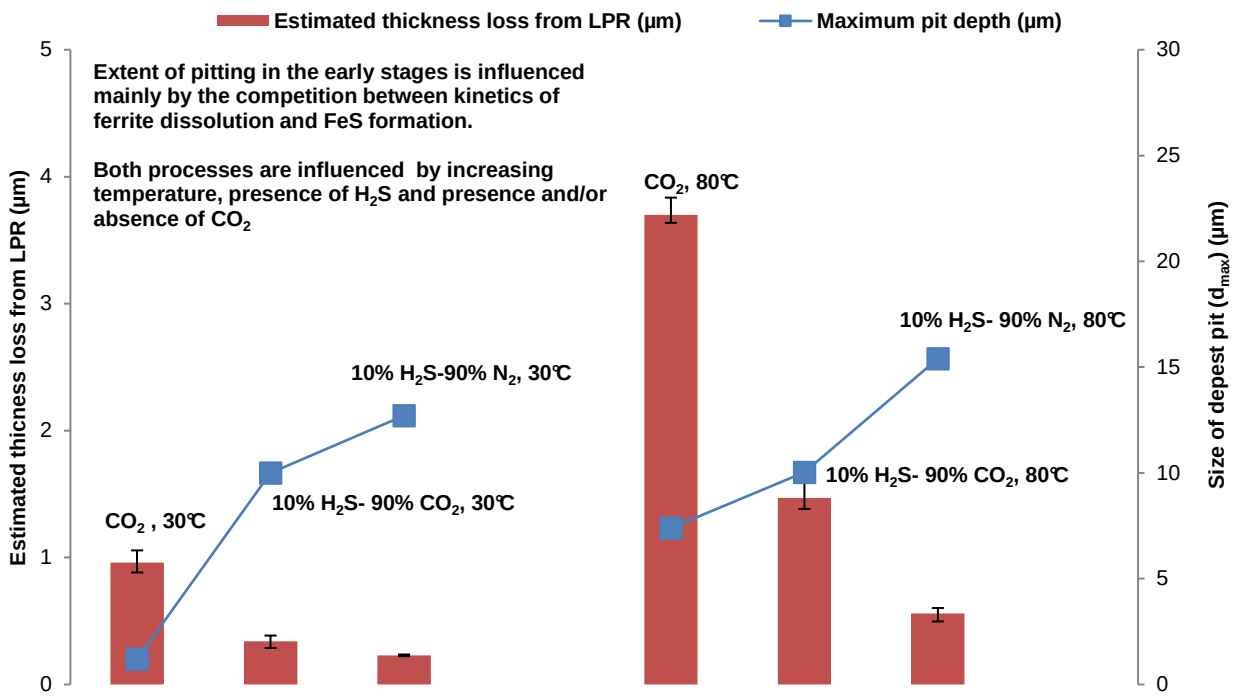

Figure 9: Summary of relationship between estimated thickness loss due to uniform corrosion and size of deepest initiated pit (relative to corroded surface) as a function of environmental parameters in H_2S-containing corrosion systems after 7 h.

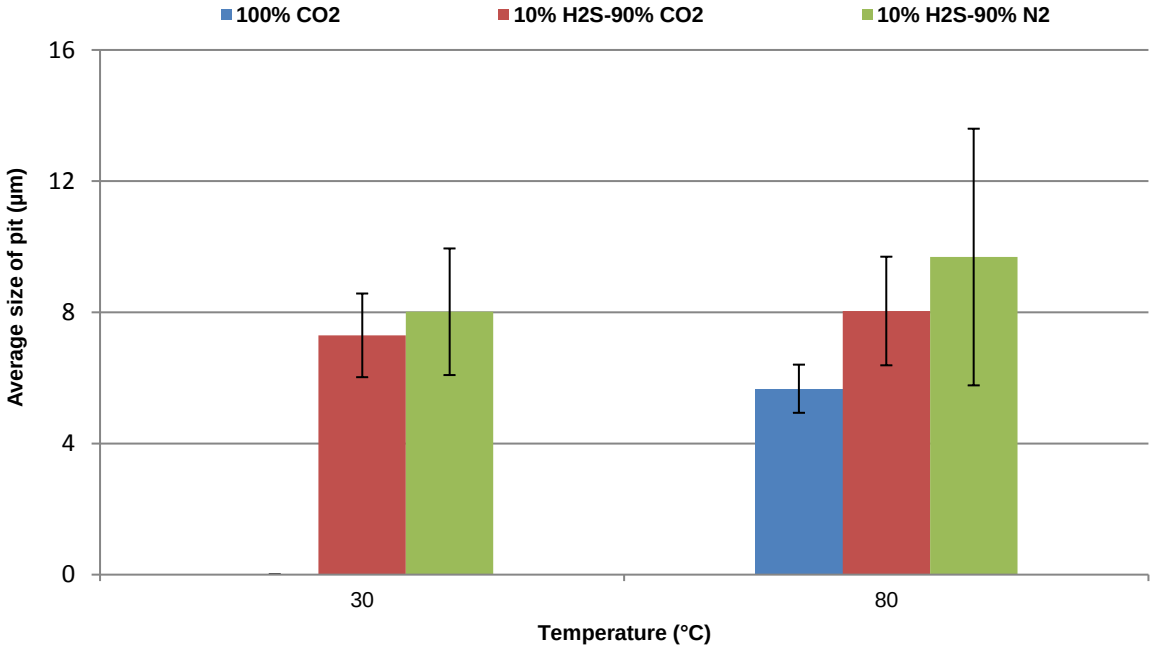

A

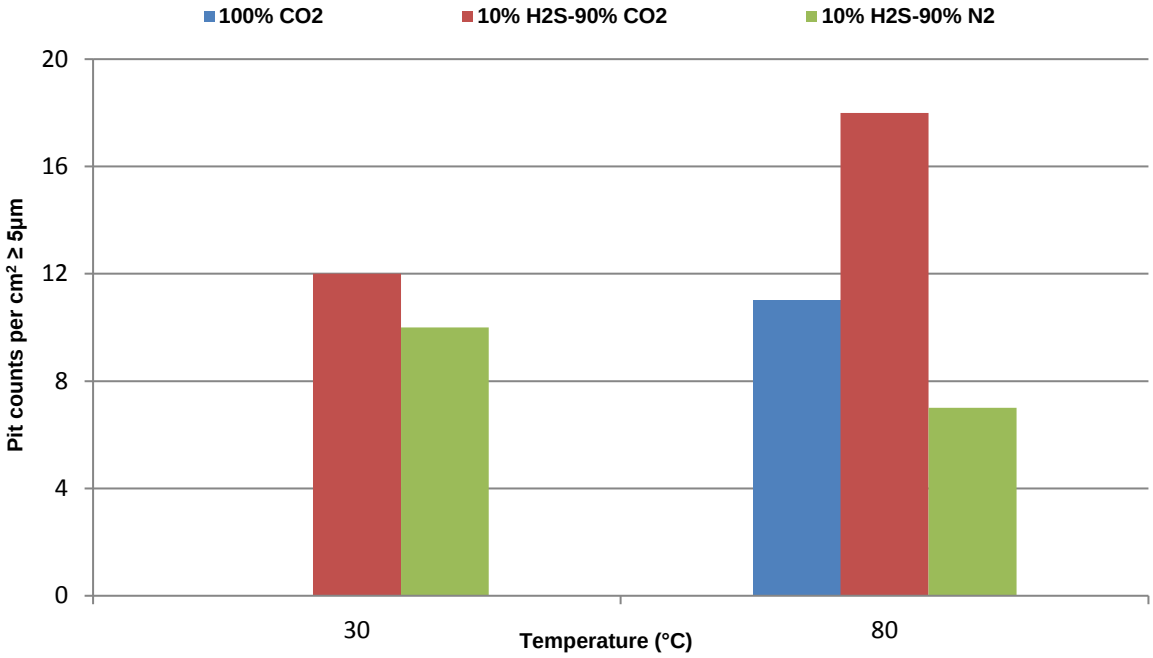

B

Figure 10: (a) Average pit depth (relative to corroded surface) and (b) Number of pits ≥ 5µm per 1 cm^2 area of carbon steel surface exposed to corrosion system under 100 mol. % CO_2, 10 mol. % H_2S – 90 mol. % CO_2 and 10 mol. % H_2S – 90 mol. % N_2 gas atmosphere as a function of temperature after 7 h. (Error bars are based on the standard deviation from the average of size of 10 deepest pit)

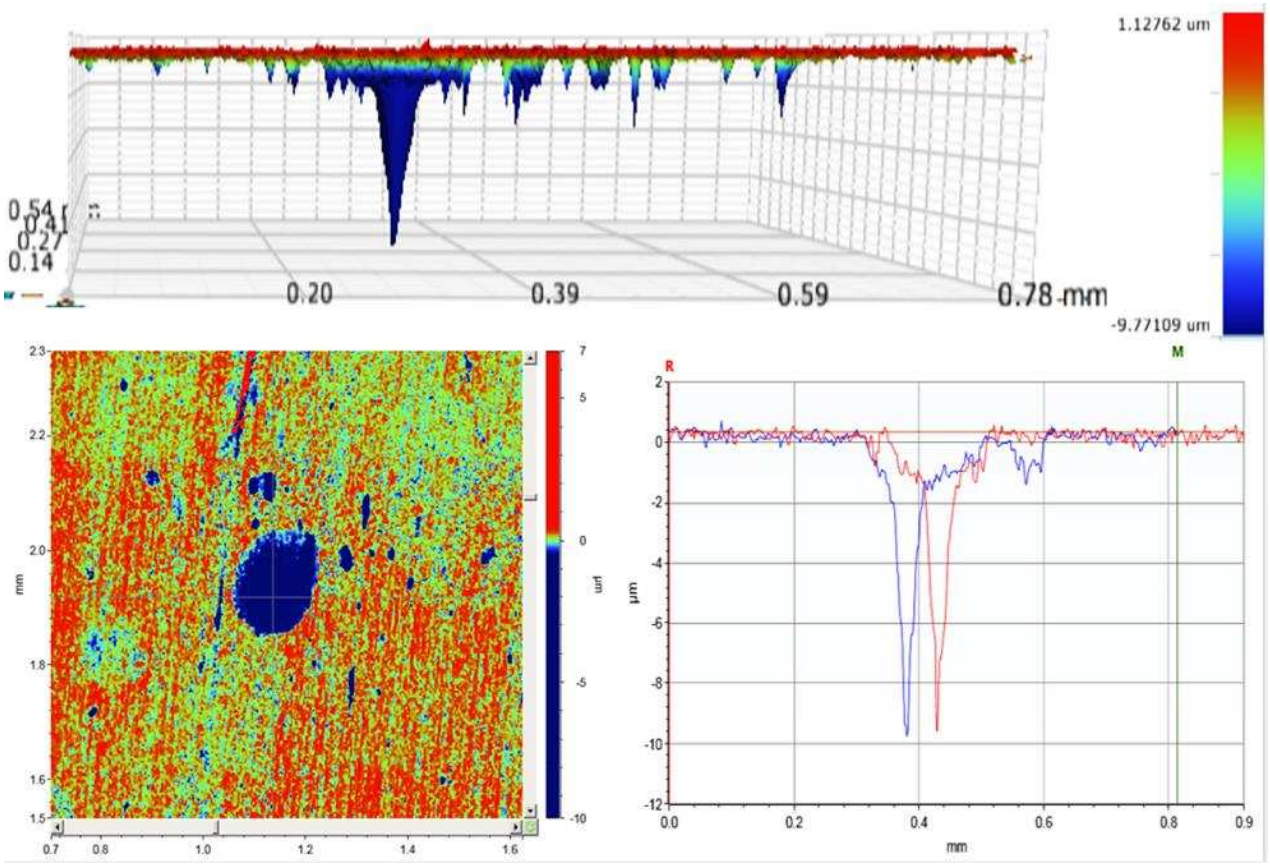

A

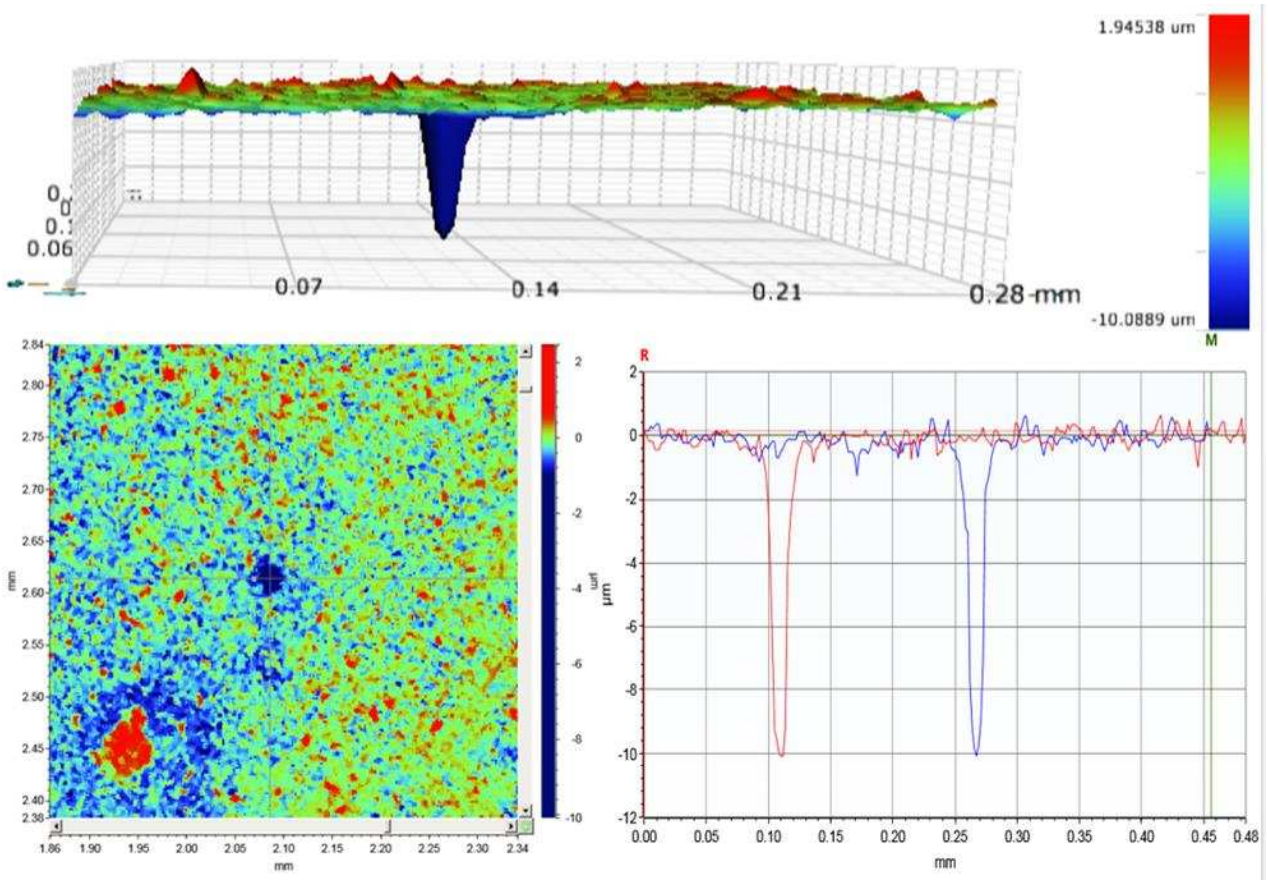

B

Figure 11: 2D and 3D images of deepest pits (relative to corroded surface) on carbon steel surface exposed to corrosion system under 10mol.% H_2S – 90 mol.% CO_2 for 7 h at (a) 30℃ and (b) 80° C.

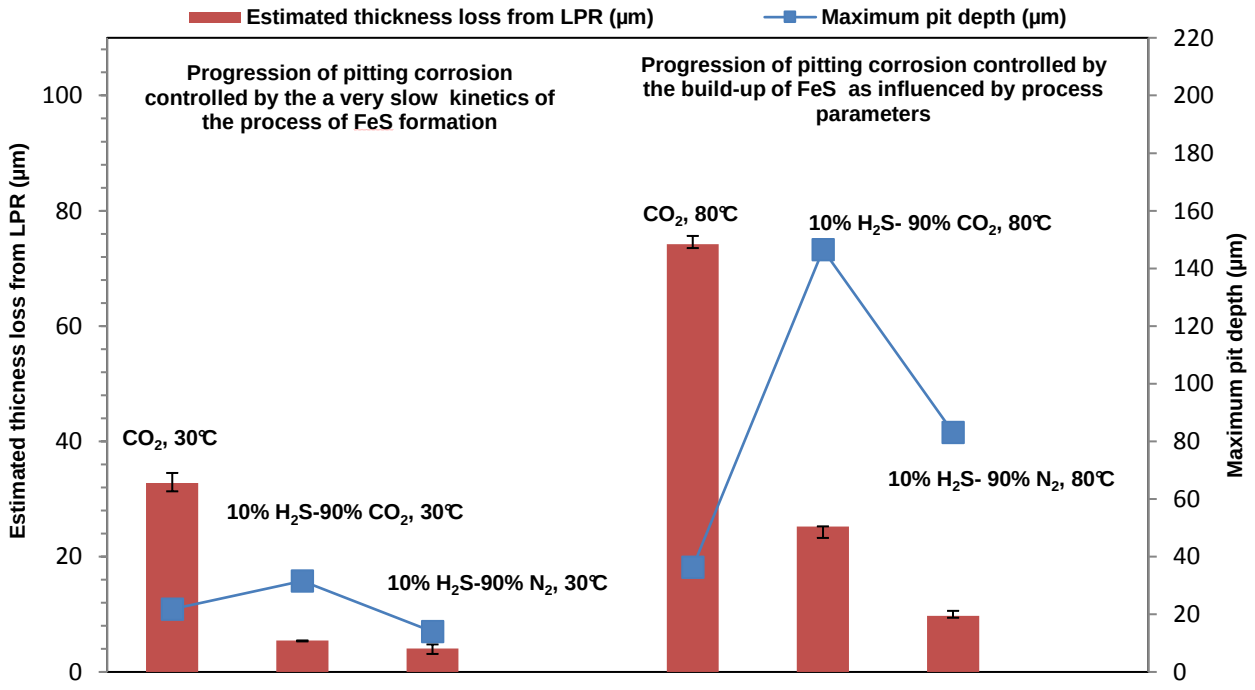

Figure 12: Summary of relationship between estimated thickness loss due to uniform corrosion and size of deepest propagated pit (relative to corroded surface) as a function of environmental parameters in H_2S-containing corrosion systems after 168 h

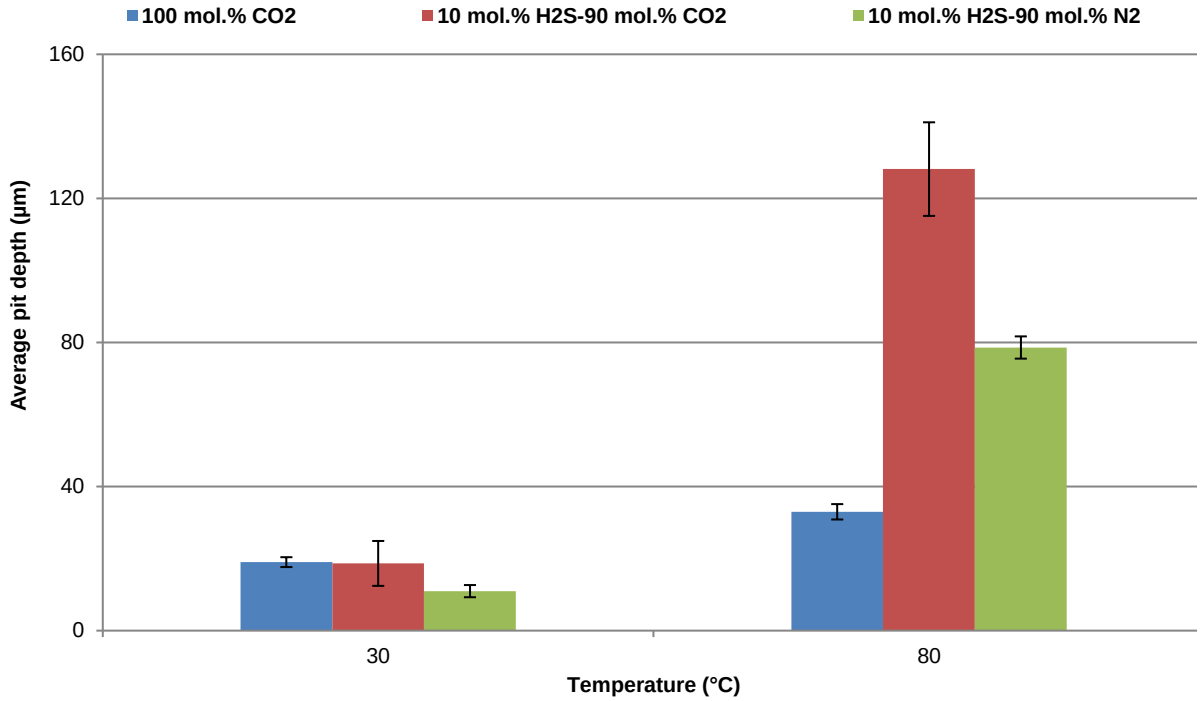

Figure 13: Average pit depth (relative to corroded surface) on carbon steel surface exposed to corrosion system under 100mol.% CO_2, 10mol.% H_2S - 90mol.% CO_2 and 10mol.% H_2S - 90mol.% N_2 gas atmosphere for 168 h as a function of temperature. (Error bars are based on the standard deviation from the average of size of 10 deepest pit)

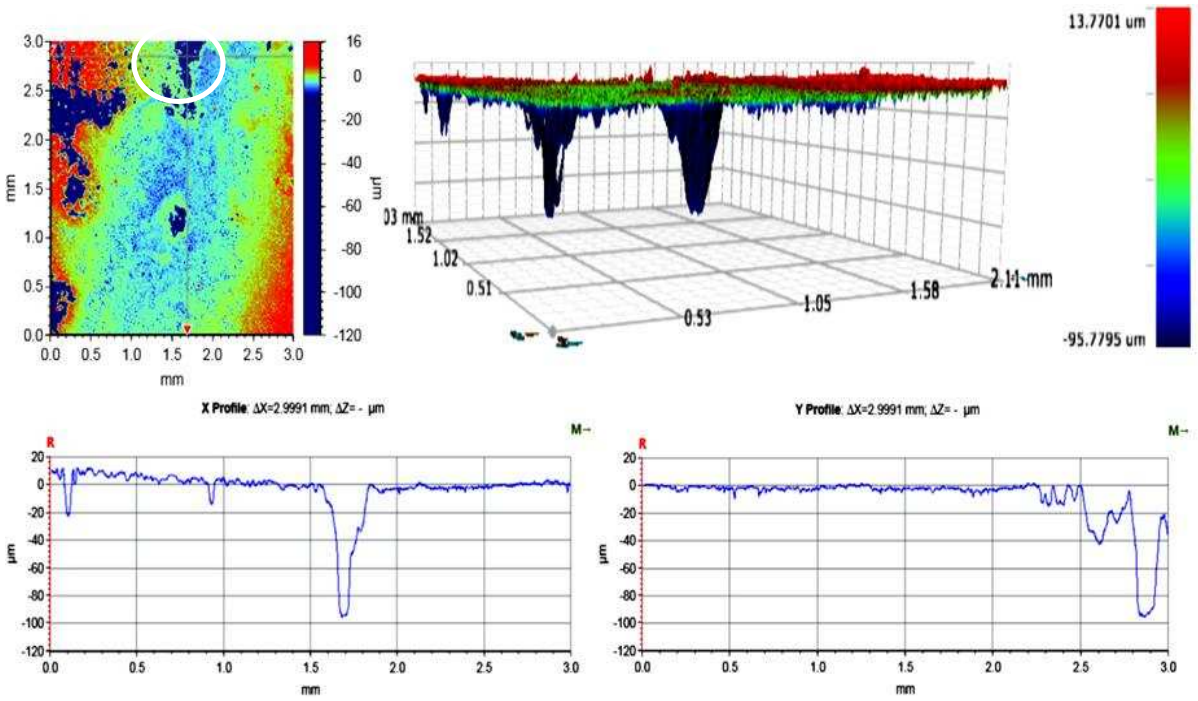

Figure 14: 2D and 3D images of deepest pit (relative to corroded surface) on carbon steel surface exposed to corrosion system under 10mole% H_2S - 90mole% CO_2 after 168 h at 80℃, after 168 h.